A critical review on surface modifications mitigating dairy fouling

Manon Saget, Caroline Françolle Almeida, Vanessa Fierro, Alain Celzard, Guillaume Delaplace, V. Thomy, Yannick Coffinier, Maude Jimenez

Received: 26 November 2020 | Revised: 18 May 2021 | Accepted: 6 June 2021

DOI: 10.1111/1541-4337.12794

COMPREHENSIVE REVIEWS IN FOOD SCIENCE AND FOOD SAFETY

Comprehensive REVIEWS in Food Science and Food Safety WILEY

A critical review on surface modifications mitigating dairy fouling

Manon Saget[1,2] | **Caroline Françolle de Almeida**[4] | **Vanessa Fierro**[4] | **Alain Celzard**[4] | **Guillaume Delaplace**[1] | **Vincent Thomy**[2] | **Yannick Coffinier**[2] | **Maude Jimenez**[1,3]

[1] Univ. Lille, CNRS, INRAE, Centrale Lille, UMR 8207 - UMET - Unité Matériaux et Transformations, Lille, France

[2] Univ. Lille, CNRS, Centrale Lille, Univ. Polytechnique Hauts-de-France, UMR 8520 - IEMN, Lille, France

[3] Institut Universitaire de France, Paris, France

[4] Univ. Lorraine, CNRS, IJL, Epinal, France

Correspondence
Maude Jimenez, Univ. Lille, CNRS, INRAE, Centrale Lille, UMR 8207 - UMET - Unité Matériaux et Transformations, F-59000 Lille, France.
Email: maude.jimenez@univ-lille.fr

Funding information
Agence Nationale de la Recherche, Grant/Award Number: ECONOMICS Project ANR-17-CE08-0032

Abstract

Thermal treatments performed in food processing industries generate fouling. This fouling deposit impairs heat transfer mechanism by creating a thermal resistance, thus leading to regular shutdown of the processes. Therefore, periodic and harsh cleaning-in-place (CIP) procedures are implemented. This CIP involves the use of chemicals and high amounts of water, thus increasing environmental burden. It has been estimated that 80% of production costs are owed to dairy fouling deposit. Since the 1970s, different types of surface modifications have been performed either to prevent fouling deposition (anti-fouling) or to facilitate removal (fouling-release). This review points out the impacts of surface modification on type A dairy fouling and on cleaning behaviors under batch and continuous flow conditions. Both types of anti-fouling and fouling-release coatings are reported as well as the different techniques used to modify stainless steel surface. Finally, methods for testing and characterising the effectiveness of coatings in mitigating dairy fouling are discussed.

1 | INTRODUCTION

Food processing industries have to respect strict hygiene and safety standards to ensure the shelf life and quality of products while avoiding contamination by microorganisms. Hence, thermal treatments such as pasteurization, sterilization or ultrahigh temperature (UHT) treatment are mandatory for dairy and its by-products. Fluids are treated at temperatures ranging from 62 to 150°C for 30 min to a few seconds (Bylund, 1995; Hagsten, 2016; Holsinger et al., 1997). However, thermal processes trigger protein denaturation and salt precipitation, leading to a fouling deposit on heat exchangers' surfaces, that poses many problems for food processing industries. Firstly, if heat exchangers' surfaces are not cleaned regularly, bacteria can

Abbreviations: AFM, atomic force microscopy; APP, atmospheric pressure plasma; CAH, contact angle hysteresis; CIP, cleaning-in-place; CVD, chemical vapor deposition; DLC, diamond-like carbon; FEP, fluorinated ethylene propylene; HMDSO, hexamethyldisiloxane; NAT, native stainless steel; PDMS, polydimethylsiloxane; PECVD, plasma enhanced chemical vapor deposition; PEG, polyethylene glycol; PEI, polyethylenimine; PEO, polyethylene oxide; PFA, perfluoroalkoxy alkane; PHE, plate heat exchanger; PTFE, polytetrafluoroethylene; SAMs, self-assembled monolayers; SFE, surface free energy; SLIPS, slippery liquid-infused porous surface; SMUF, simulated milk ultrafiltrate; SS, stainless steel; ToF-SIMS, time-of-flight secondary ion mass spectroscopy; UHT, ultrahigh temperature; WCA, water contact angle; WPC, whey protein concentrate; WPI, whey protein isolate; XPS, X-ray photoelectron spectroscopy; β-Lg, β-lactoglobulin.

accumulate on the surface creating biofilms on it (Bott, 2011; Hinton et al., 2002; Marchand et al., 2012). Secondly, fouling deposits impair heat transfer mechanisms by creating a thermal resistance leading to regular shutdown to clean the processes.

304 and 316L stainless steels (SSs) are mostly used in food processing industries due to their properties such as high physical durability, chemical neutrality and cleanliness. In food industries, SS surfaces should present arithmetic mean roughness (R_a) < 0.8 μm (Verran & Redfern, 2016) and several types of finish exist. This can lead to surfaces with various physical and chemical properties (Hall, 1939; Schmidt et al., 2012). Regardless of the durability and cleanliness of these types of SS, food processing plants have to be cleaned every day to prevent contamination risks (Lalande et al., 1989). Therefore, harsh cleaning-in-place (CIP) procedures are implemented. CIP involves the use of chemicals and high amount of water, which increases the environmental burden. It is estimated that 80% of production costs are owed to dairy fouling deposit (Van Asselt et al., 2005).

In food industries, the fouling step can be defined as the increase of thickness of the fouled layer onto SS surface heat exchanger. Thus, cleaning step corresponds to the decrease of the thickness of this fouled layer. The increase of thickness of fouled layer corresponds to fouling and thus the decrease of this layer corresponds to cleaning. These both steps (fouling and cleaning) are determined by measuring the thermal fouling resistance (R_f) and the pressure drop (Δp). The thermal fouling resistance is related to the overall clean heat transfer coefficient (U_0) and to that after fouling (U_f) through the following equation:

$$R_f = \frac{1}{U_f} - \frac{1}{U_0}. \quad (1)$$

The pressure drop can be related to the mass of fouling deposit onto tubular or plate heat exchanger (PHE) surface. When fouling grows, the cross-sectional area decreases, limiting the product flow and leading to an increase of the pressure drop (Changani et al., 1997; Hagsten, 2016; Schnöing et al., 2020).

1.1 | Dairy fouling

Dairy fouling is a complex phenomenon and numerous parameters have to be considered. First of all, the milk's composition itself, which is a biological fluid containing proteins (whey proteins and caseins), lipids, soluble sugars, and mineral species. Moreover, the milk's composition can vary as a function of the season and of its source (Burton, 1967). It is also important to note that, depending on filtration processing, the whey proteins, casein, and mineral contents are thus modified, leading to different fouling mechanisms (Blanpain-Avet et al., 2020; Liu et al., 2020).

Secondly, it has been observed that the composition of milk fouling deposit differs significantly from that of raw milk. Milk fouling deposit is mainly composed of whey proteins and minerals. Caseins, lactose and fat seem to be negligible in milk fouling deposit, although they represent 80% of soluble compounds in milk (Jeurnink et al., 1996; Lalande & René, 1988; Lyster, 1965; Visser & Jeurnink, 1997).

Furthermore, depending on the temperature to which dairy products are exposed (Table 1), fouling deposits have been classified into two categories. The first one, called Type A, gathers proteinaceous deposits formed at temperatures ranging from 75 to 100°C. This deposit is white, slightly dense, spongy, and mostly composed of proteins (50%–60%), more precisely of β-lactoglobulin (β-Lg) (Lalande et al., 1985; Tissier & Lalande, 1986), minerals such as calcium phosphate (30%–35%) and lipids (5%). On the contrary, the second one, called Type B, gathers mineral fouling that builds up at higher temperatures, at 105°C. This type of deposit is grey, denser, and rougher and mainly composed of mineral species, calcium phosphate (70%), proteins (20%), and lipids (5%) (Burton, 1968; Hagsten et al., 2016).

At pilot scale (about 300 L/hr), the use of fresh raw milk is expensive and its storage can be complicated.

Moreover, being a natural fluid, its chemical composition may vary, leading to differences in fouling experiments. For this reason, reconstituted milk solutions from whey protein concentrate (WPC) or whey protein isolate (WPI) have been used to achieve reproducible fouling behavior (Delplace et al., 1997; Lalande et al., 1985). WPC and WPI are obtained from milk filtration. This process is widely used to separate caseins from whey proteins as both of these proteins have specific properties which can be used for diverse food applications (Carter et al., 2021; Smithers et al., 1996). It has been demonstrated that fouling deposit from WPC solution mimics well fouling deposit type A from milk at pasteurization temperatures (42–120°C). However, at UHT temperatures (120–134°C) fouling deposit from WPC is mainly composed of whey proteins, whereas fouling deposit from milk is mainly composed of mineral salts (Robbins et al., 1999). Therefore, in most investigations, WPC or WPI solutions with simulated milk ultrafiltrate (SMUF) or calcium and phosphate are used as model fluid mimicking milk.

According to the literature, the proteinaceous fouling deposit (Type A) leads to greater issues for food processing plants than type B fouling deposit. Being less dense, type A fouling deposit increases the pressure drop and thermal resistance and is less easy to remove than type B

TABLE 1 Table of legal pasteurization standards (adapted from Bylund, 1995; Hagsten, 2016; Holsinger et al., 1997)

Process type	Time	Temperature (°C)	Type of fouling (Burton's classification)
Batch pasteurization (low temperature for a long time)	30 min	63	A
High-temperature, short-time pasteurization	15–20 s	72–75	A
Ultrapasteurization	2–4 s	125–138	A up to 100°C B from 110°C
UHT treatment	Few seconds	134–150	B

fouling deposit (Burton, 1968; Fickak et al., 2011; Lyster, 1965; Van Asselt et al., 2005). Type A fouling deposit has been therefore more studied. Thus, this review will focus on this fouling deposit formed in pasteurization temperature range (<100°C) and will not deal with type B fouling deposit.

1.2 | Dairy fouling mechanisms

Based on the previous section, two major components of milk are responsible of the growth of fouling deposit onto heat exchangers' surfaces. Whey proteins and notably β-Lg proteins and calcium phosphates are thermosensitive; therefore, heat induces denaturation and/or aggregation of whey proteins and precipitation of calcium phosphates in bulk solution and onto heat exchanger's surfaces.

It has been demonstrated that whey proteins are the most thermosensitive proteins in milk. Moreover, Polat (2009) showed that β-Lg proteins denature faster than α-lactalbumin protein in pasteurization temperature range. Therefore, β-Lg proteins are the main component of type A fouling deposit. When the temperature increases and reaches 65°C, β-Lg becomes thermally unstable, leading to its denaturation and thus exposing reactive thiol groups. These reactive groups tend to achieve intramolecular polymerisation either with other β-Lg or other proteins (α-lactalbumin) via disulphide bonds (De Wit, 1990; Hoffmann & Van Mil, 1997). Nevertheless, reactive thiol groups are not the only impacting factor, and several investigations reported the role of calcium ions in the interactions between proteins and whey protein denaturation/aggregation (Belmar-Beiny & Fryer, 1993; Guérin et al., 2007; Petit et al., 2011).

In parallel, calcium phosphates are less soluble with the increase of temperature. This decrease of solubility leads to nucleation and crystal growth in the bulk and onto heat exchangers' surfaces. Delsing and Hiddink (1983) demonstrated that calcium ions play also a great role in the fouling growth. This has been confirmed by Jimenez et al. (2013) who pointed out fouling growth mechanisms in the presence or absence of calcium. In the absence of calcium, the substrate and the steel grain boundaries are covered with a very thin layer of whey proteins as displayed in Figure 1 (left). In the presence of calcium, large-size particles are observed on the protein layer, leading to an arborescent structure.

According to the literature, several investigations, reported in different reviews (Bansal & Chen, 2006; Sadeghinezhad et al., 2015; Sadeghinezhad et al., 2013), have studied the mechanisms of milk fouling. Today, it is well accepted that an initial phase – also called induction period – takes place, where a thin layer forms onto heat exchangers' surfaces before the fouling deposit is noticeable. During this initial phase, no changes in pressure drop and heat transfer coefficient are observed (Fryer & Belmar-Beiny, 1991; Fryer & Christian, 2005). The duration of this induction period varies generally from 1 to 60 min in tubular heat exchangers and is often instantaneous in PHEs (Belmar-Beiny & Fryer, 1993; De Jong, 1997).

The composition of the thin first layer has been debated for a long time. Some authors observed a thin layer mainly constituted of calcium phosphate after 1–15 min of fouling test at pasteurization temperature (Foster & Green, 1989; Fryer & Belmar-Beiny, 1991; Tissier & Lalande, 1986). Nevertheless at shorter time (4 s), Belmar-Beiny et al. (1993) showed, thanks to X-ray elemental mapping, X-ray photoelectron spectroscopy (XPS), and scanning electron microscopy, that the first layer was mainly composed of whey proteins, allowing the fouling to grow. This has been corroborated by Jimenez et al. who performed fouling runs for 1 min. They observed by time of flight-secondary ion mass spectrometry (ToF-SIMS) that the substrate and the steel grain boundaries were covered with a homogeneous layer of whey proteins and the Ca^{2+} ions were concentrated in the upper side of the fouling deposit (Jimenez et al., 2013).

In the meantime, Belmar-Beiny et al. (1993) carried out investigations for longer time (60 min) and highlighted a higher concentration of calcium phosphate near the heated surface (in the boundary layer). This corroborates

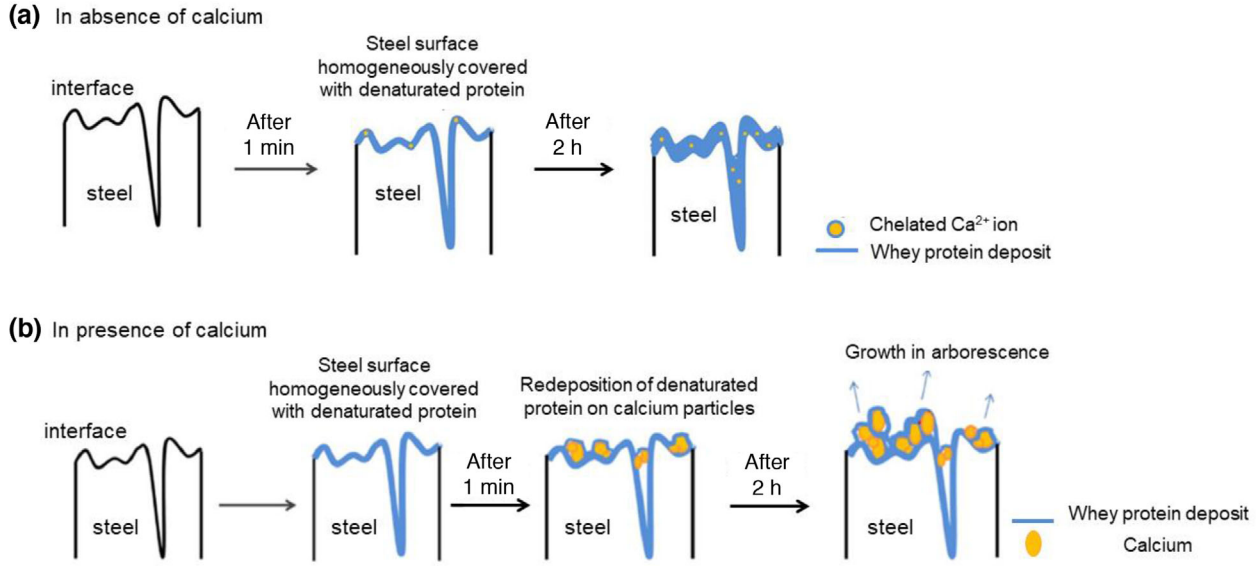

FIGURE 1 Fouling growth mechanisms (a) in the absence of calcium and (b) in the presence of calcium (Jimenez et al., 2013)
Note: Reprinted with permission from Elsevier B.V.

the observations made by Jimenez et al. after 120 min and by Tissier and Lalande after 240 min.

Fouling deposition relies on simultaneous and/or successive phenomena which have been gathered in different stages described and reviewed by Bansal and Chen (2006), Belmar-Beiny et al. (1993), Bohnet (1987) and Epstein (1983):

1. Bulk activation: denaturation and/or aggregation of whey proteins in bulk solution;
2. Transport/mass transfer: transport of denatured and/or aggregated whey proteins and calcium and phosphate ions to the heat surface;
3. Surface reactions: adsorption of denatured/aggregated whey proteins, calcium and phosphate ions initiating the fouling and leading to the fouling growth via the incorporation and entrapment of denatured/aggregated whey proteins, calcium and phosphate ions and particulates;
4. Aging of the fouling deposit: deposit removal and transfer of denatured/aggregated whey proteins and calcium and phosphate particulates back to the bulk solution (re-entrainment).

1.3 | Factors impacting dairy fouling

According to the literature, numerous factors affect the formation of dairy fouling. These factors are gathered in three main groups: (i) product characteristics, (ii) process parameters and (iii) surface properties displayed in Figure 2 (Zouaghi, 2018). For each group, Boxler (2014) reported the trends of the effect of different factors impacting milk fouling.

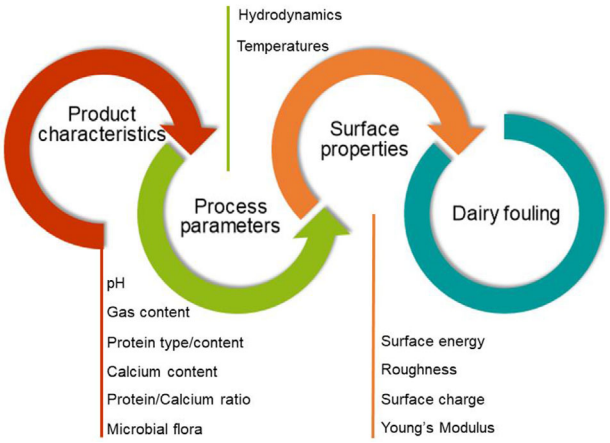

FIGURE 2 Three categories of factors affecting dairy fouling (adapted from Zouaghi, 2018)

Förster et al. (1999) demonstrated that fouling mitigation could be managed by two pathways. The first one consists in modifying the geometry and surface properties of heat exchanger surface to reduce the deposit adhesion. The other one consists in increasing flow rate in order to increase wall shear stress inducing fouling deposit removal. This latter approach to mitigate fouling deposit has been corroborated by Mahdi et al. (2009). However, fouling occurs at the interface between the surface and the liquid phase. Thus, the surface properties play also an important role in fouling behavior (Bohnet, 1987).

Therefore, this review only focuses on the impact of surface modification on fouling and cleaning behavior. Surface properties used to characterize coatings and materials are described in the next section. Numerous investigations have reported the impact of surface properties onto fouling deposit; however, the comparison between these works is difficult. Indeed, fouling tests were performed using various model fluids, process types, and conditions. Hence, in the subsequent section, studies are divided as function of the process type, that is, batch or continuous flow pasteurization. This will lead to establish the influence of surface properties on fouling behavior and to explain how surface modifications are performed. Some authors also investigated the cleanability of modified surfaces, leading to the distinction between anti-fouling and fouling-release surfaces in a third part. Finally, process parameters of fouling test, surface characterizations and cleaning conditions will be discussed to make the comparison between investigations on surface modifications more relevant. A standardization of surface characterizations and cleaning conditions is then proposed based on different investigations.

2 | SURFACE PROPERTIES

The induction phase can be seen as the most important step in fouling mechanisms. Indeed, during this short time, the adsorption of whey proteins to heat exchanger surfaces takes place, leading to further adhesion of minerals and whey proteins. Adsorption and adhesion phenomena are governed by physicochemical interactions at the interface. These interactions influencing adsorption and adhesion can be divided into two groups: (i) mechanical interactions and (ii) molecular interactions. Mechanical interactions gather roughness and topography. Molecular interactions include several forces corresponding to the surface energy parameter (Boxler, 2014; Schnöing et al., 2020).

2.1 | Mechanical interactions: Roughness and topography

Surface roughness in an important parameter acting on (i) thermal processing performances and (ii) dairy fouling mechanisms. Rough surfaces lead to an increase of heat transfer and turbulence and thus an increase of mass transfer (Albert et al., 2011; Schnöing et al., 2020). On the other hand, rough surfaces are more prone to fouling due to a larger available area (grain boundaries) (Boxler, 2014; Jimenez et al., 2013; Zouaghi et al., 2018).

Nonetheless, the calculation of the real surface geometry is complex, and Gadelmawla et al. (2002) reported around 60 roughness parameters gathered in three different groups: amplitude parameters, spacing parameters and hybrid parameters. Surface topography is often characterized by amplitude parameters measuring the vertical surface deviations. Especially, the arithmetic average height (R_a) or centre line average and the root mean square roughness (R_q or RMS) are the most used roughness parameters. R_a (Equation 2) represents the absolute average of vertical surface deviations from the mean centre line over length range (Figure 3). R_q (Equation 3) describes the standard deviation of the distribution of surface heights:

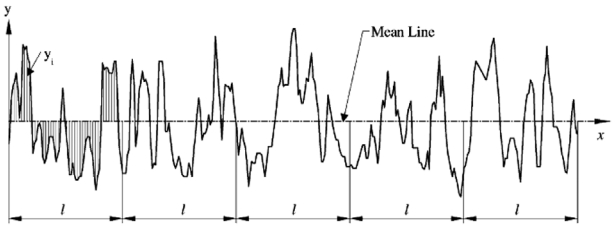

FIGURE 3 Representation of the arithmetic average height (R_a) (Gadelmawla et al., 2002)
Note: Reprinted with permission from Elsevier B.V.

$$R_a = \frac{1}{n}\sum_{i=1}^{n} |y_i|\,, \tag{2}$$

$$R_q = \sqrt{\frac{1}{n}\sum_{i=1}^{n} Z_i^2}. \tag{3}$$

Different techniques exist to measure the surface topography driving to R_a parameter, namely, profilometer, atomic force microscopy (AFM), coherence scanning interferometry, and confocal microscopy (Magens, 2019).

2.2 | Molecular interactions: Surface free energy

The adhesion of whey proteins and calcium phosphates can be explained by the theory developed by Derjauin and Landau (1941) and Verwey and Overbeck (1948), called DLVO theory from the names of their inventors. According to this DLVO theory, attractive Lifshitz–van der Waals forces and repulsive double layer trigger the attachment phenomenon. However, the DLVO theory has been extended by taking into account the Lewis acid/base forces (hydrophilic repulsion and hydrophobic attraction) and the Brownian motion (Al-Janabi et al., 2010; van Oss, 1995). Therefore, the total interaction energy between the fouling deposit and the solid substrate (Equation 4) is constituted of Lifshitz–van der Waals, electrostatic, and the

TABLE 2 Empirical models for SFE calculation (Zouaghi, 2018)

Name	Component	Model	References
Zisman	One	Measuring several probe liquids' CA and plot the cosine of those angles against the known surface energies, then extrapolate to contact angle equal 0.	Zisman, 1964
Owens, Wendt, Rabel and Kaelble (OWRK)	Two	$\frac{\gamma_L(\cos\theta+1)}{2\sqrt{\gamma_L^D}} = \frac{\sqrt{\gamma_S^P}\sqrt{\gamma_L^P}}{\sqrt{\gamma_L^D}} + \sqrt{\gamma_S^D}$	Kaelble, 1970; Owens & Wendt, 1969
Wu	Two	$\gamma_{SL} = \gamma_S + \gamma_L - 4\left[\frac{\gamma_S^D\gamma_L^D}{(\gamma_S^D+\gamma_L^D)} + \frac{\gamma_S^P\gamma_L^P}{(\gamma_S^P+\gamma_L^P)}\right]$	Wu, 1973
Van Oss, Chaudhury and Good	Three	$\gamma_L(1+\cos\theta) = 2\left[\sqrt{\gamma_L^{LW}\gamma_S^{LW}} + \sqrt{\gamma_L^+\gamma_S^-} + \sqrt{\gamma_L^-\gamma_S^+}\right]$	van Oss et al., 1988

short-range (Lewis acid/base interactions and Brownian motion) interactions as detailed in the following, where 1, 2, and 3 indicate the fouling deposit, substrate, and liquid, respectively,

$$\Delta G_{1,2,3}^{TOT} = \Delta G_{1,2,3}^{LW} + \Delta G_{1,2,3}^{EL} + \Delta G_{1,2,3}^{AB} + \Delta G_{1,2,3}^{Br}. \quad (4)$$

Nevertheless, the electric double layer repulsion and repulsive forces arising from Brownian motion can be neglected as they are too small to satisfy the balance with attractive Lifshitz–van der Waals and Lewis acid/base forces (Fowkes, 1964; Grasso et al., 2002; van Oss et al., 1987). The electric double layer repulsion decays spatially with the characteristic Debye length. In milk, this length is approximately 1 nm, thus the electric double layer interactions decrease by about 37% within the first nanometre (Magens, 2019; van Oss, 2003; Walstra et al., 2005). Consequently, Equation (4) can be simplified as follows:

$$\Delta G_{1,2,3}^{TOT} = \Delta G_{1,2,3}^{LW} + \Delta G_{1,2,3}^{AB}. \quad (5)$$

2.2.1 | Surface free energy measurement

According to van Oss, the surface free energy (SFE) of a solid substrate can be written as the sum of Lifshitz–van der Waals and Lewis acid/base interactions expressed in J/mš or N/m:

$$\gamma_i = \gamma_i^{LW} + \gamma_i^{AB}. \quad (6)$$

Other empirical models exist (Table 2). To calculate the SFE, the Owens, Wendt, Rabel, and Kaelble (OWRK) model decomposes it into polar (γ^P) (Lewis acid/base interactions) and dispersive (γ^D) parts (Lifshitz–van der Waals interactions). To go further, the van Oss, Chaudhury, and Good's model permits to split the polar part into an acid or electron acceptor component (γ^+) and a basic or electron donor component (γ^-) as follows:

$$\gamma_i^{AB} = 2\sqrt{\gamma_i^+\gamma_i^-}. \quad (7)$$

The SFE of a surface can be directly determined using the Young equation (Equation 8), where θ is the contact angle between the liquid and the solid phase, γ_{SV} is the solid–vapor interfacial energy, γ_{SL} the solid–liquid interfacial energy, and γ_{LV} the liquid–vapor interfacial energy (Young, 1804):

$$\gamma_{LV} \times \cos\theta = \gamma_{SV} - \gamma_{SL}. \quad (8)$$

The use of at least three liquids with known surface tension allows determining the SFE of a solid substrate.

2.2.2 | Wettability

The Young equation (Equation 8) is the first wetting model allowing to characterise the surface wettability, by measuring the water contact angle (WCA) between the liquid and the surface. The contact angle describes the balance of cohesive (between the molecules of the liquid) and adhesive (between the liquid and the solid) forces precisely located at the triple line (liquid/surface/air interface). Therefore, if the liquid spreads on the surface it means that the surface has a high affinity for water (cohesive forces < adhesive forces). Contrary to a wetting surface, a surface which has no affinity with the dropped liquid will repel it (cohesive forces > adhesive forces) (van Oss, 2006).

Nevertheless, the Young equation does not take into account the surface topography. It states that SFE of a smooth and homogenous surface depends on molecular interactions only. Surfaces can present irregularities and defects; thus, Wenzel rewrote the Young equation,

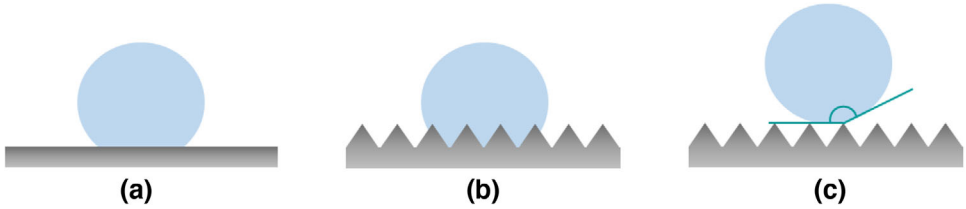

FIGURE 4 Representation of (a) a smooth hydrophobic solid surface, (b) a rough hydrophobic surface in homogeneous regime (Wenzel) and (c) a rough superhydrophobic surface in heterogeneous regime (Cassie–Baxter)

connecting both wettability and surface roughness:

$$\cos\theta^* = r\cos\theta, \tag{9}$$

where 'r' has been introduced as the 'roughness factor' which represents the ratio of actual surface to geometric surface, θ* as the apparent angle (experimental measurement) and θ as the real angle (corresponding to the contact angle of a flat surface). According to Wenzel, owing by the increased surface roughness, both solid–liquid and solid–vapor interfacial surface tensions increase slightly, but liquid–vapor interfacial surface tension does not vary. Consequently, apparent WCA is slightly greater than the real WCA (Jeevahan et al., 2018). If the perfectly flat surface is hydrophobic (hydrophilic), the corresponding roughened surface will be superhydrophobic (superhydrophilic) (Bormashenko, 2009; Wenzel, 1936).

Later, in 1944, the Wenzel equation has been further modified. Cassie and Baxter (1944) have observed that water does not necessary fill in the porous solid surface, creating liquid–vapor interface: the Cassie–Baxter equation takes into account the solid fraction in contact with water, expressed as ϕ_S (Equation (10)) (Jeevahan et al., 2018):

$$\cos\ \theta^* = -1 + \phi_S(\cos\theta + 1). \tag{10}$$

Hence, Wenzel model refers to homogeneous regime where water droplet fills up the roughness grooves and Cassie–Baxter model refers to heterogeneous regime where water droplet lies on top of the protrusions and air bubbles are trapped between water and the protrusions as displayed in Figure 4 (Jeevahan et al., 2018; Yan et al., 2011)

2.2.3 | Contact angle hysteresis

However, the parameters r and ϕ_S, which distinguish Wenzel model from Cassie–Baxter model, are complex to quantify. Therefore, to discriminate these two superhydrophobic states the measurement of contact angle hysteresis (CAH) is performed. It has been demonstrated that Wenzel state drives to high CAH because the droplet is sticked to the surface. On the contrary, a quasi-null hysteresis is observed in Cassie–Baxter state due to the sliding of the droplet (Yan et al., 2011).

The CAH parameter can be measured using two different methods: the volume variation of the droplet or the tilting plate.

The first one consists slowly pumping the liquid into and out of the droplet giving the advancing and receding angles. The second one consists tilting the surface where the drop is standing. When the surface is tilted, water droplet undergoes both surface tension and gravity. The drop starts to slide as illustrated in Figure 5 and becomes asymmetric achieving the advancing and receding angles. Advantages and drawbacks of these two methods have been reviewed by Eral et al. (2013).

CAH can thus be calculated thanks to the Equation (11), where θ_h is the CAH, θ_a is the advancing contact angle at the lower side and θ_r is the receding contact angle at the upper side:

$$\theta_h = \theta_a - \theta_r. \tag{11}$$

The higher the difference is, the more the droplet will be pinned on the surface. On the contrary, the lower the difference is, the more the droplet will be repelled (Eral et al., 2013; McHale et al., 2004).

3 | SURFACE MODIFICATIONS TO MITIGATE DAIRY FOULING DEPOSIT

Studies on surface modifications to mitigate dairy fouling deposit started in 1968 and extended greatly in the 1990s. Modifying the surface is one of the two pathways mitigating dairy fouling deposit. Heat exchangers' surfaces have been modified in order to make the induction period longer. Indeed, a longer induction phase would enhance heat exchangers' operating efficiency leading to less frequent or less harsh cleaning (Boxler, 2014; Förster et al., 1999). In 2015, a study (Gomes Da Cruz et al., 2015) showed that surface modifications could be economically attractive as long as coatings could extend the duration of

FIGURE 5 Receding and advancing contact angles determining contact angle hysteresis

pasteurization period, reduce cleaning and conserve heat transfer efficiency.

Surface modifications allow to physically or chemically change the surface properties of a material. They are performed via different techniques, which will be presented in Section 3.2. The literature gathers about 50 studies on the impact of modified surfaces on dairy fouling. Nevertheless, the comparison remains complex due to several reasons. First of all, milk can be pasteurized under various conditions: (i) batch pasteurization, (ii) high-temperature, short-time pasteurization and (iii) UHT pasteurization (Table 1); consequently, some studies have been performed in batch and other in continuous flow mimicking high-temperature, short-time pasteurization (Holsinger et al., 1997).

Secondly, different process parameters (bulk and surface temperatures and hydrodynamic regime) are used for fouling runs, either in batch or in continuous flow. Indeed, the fouling layer growth is not similar in batch and continuous flow conditions. When the liquid to be processed passes through the heated channel once, the composition of the processed fluids (in native, unfolding and aggregated proteins species…) feeding the fouling layer is fixed. This means that the deposit build-up happens in steady conditions. On the contrary, when the liquid to be processed passes through the heated channel many times, the composition of the foulant fluids fluctuates with time. It means that the formation of the deposit occurs this time in unsteady conditions. Indeed, there is a depletion in native proteins species and a loss of precursor species (unfolded or aggregated species) as the number of passing through the heat exchanger increases.

In some cases, after the fouling run, rinsing and/or cleaning steps are carried out. The latter rinsing step reveals whether the surface helps fouling removal along. This type of surface will be referred to as a fouling-release surface in opposition to an anti-fouling surface that remains un-fouled after a pasteurization cycle. Finally, the surface properties (wettability and/or SFE and/or roughness) are not always assessed. Therefore, among the publications on surface modifications, the focus will be on experiments carried out in batch or continuous flow conditions using SS as surface reference and presenting surface characterizations of coated surfaces. In these investigations, fouling is quantified by weighing the deposit, measuring the pressure drop or calculating the thermal fouling resistance through the overall heat transfer coefficients of the soiled and cleaned surfaces.

3.1 | Impact of surface properties on dairy fouling

3.1.1 | Batch pasteurization

The fouling mechanism under batch conditions differs from that of a continuous flow in a heat exchanger. The flow regime, mass and heat transfer and bulk temperature are indeed not comparable. According to the literature, some studies were realized in laminar regime, with shear stress (Britten et al., 1988; Mauermann et al., 2009; Rosmaninho & Melo, 2006). Boxler et al. (2013a) performed fouling test in a stirrer tank rotating at 60 rpm, corresponding to a Reynolds number of 12,360, which is in the range of turbulent flow under batch conditions. At this flow regime, fouling deposit removal was observed due to the weak adhesion of the particles onto the surface (Boxler, 2014; Boxler et al., 2013). In dairy industries, batch pasteurizations are performed at around 63°C (Holsinger et al., 1997), which is slightly lower than the denaturation temperature of β-Lg (70–74°C). Thus, β-Lg proteins are not supposed to form aggregates in the bulk; however, when the surface is heated, denaturation can take place near it, in the boundary layer. Consequently, according to Boxler (2014), β-Lg can either adsorb on the surface and denature or denature in the boundary layer and then adsorb on the surface. With a high temperature difference between bulk and heated surface, no additional β-Lg aggregates form on the surface. According to Itoh et al. (1995), aggregation of β-Lg can occur close to the surface (in the boundary layer) but these aggregates barely adhere to the surface. At high temperature, β-Lg first denatures on the surface and then can aggregate to other denatured β-Lg proteins. Therefore, under batch conditions, fouling rate depends on surface reactions and thermal boundary layer.

With these considerations in mind, batch studies are separated from those in continuous flow and are gathered in Table 3 adapted from Boxler (2014) and Zouaghi (2018).

TABLE 3 Impact of surface properties on fouling behaviour in batch conditions, adapted from (Boxler, 2014; Zouaghi, 2018)

Investigated parameter	Observations	Coating/Surface	[a]SFE, [b]γ^+, [c]γ^- (mN/m)	WCA (°)	R_a (μm)	Tested fluid	Tested parameters	Rinsing/ cleaning parameters	Reference
Surface free energy (SFE)	An optimal SFE value allows to reduce protein adsorption	Standard 304 SS	78.4[a]/38.3[b]	–	–	β-Lactoglobulin in phosphate buffer solution (PBS)	Batch (360 min) T_{bulk} = 30°C		Kirtley & McGuire, 1989
		Glass	159[a]/127[b]	–	–				
		Nylon	87.6[a]/47.5[b]	–	–				
		PE HD	60.4[a]/22[b]	–	–				
		PE	47.9[a]/12[b]	–	–				
		PP	68.5[a]/29.7[b]	–	–				
		PTFE	22.6[a]/0[b]	–	–				
	Low SFE improves the cleanability	304 AISI SS	38.3[a]/6.6[b]	–	0.15	WPI in water	Batch T_{bulk} = 60–80°C	2% NaOH solution spray Water spray	Mauermann et al., 2009
		Nanocomposite I	23.6[a]/2.4[b]	–	0.07				
		Nanocomposite V	29.8[a]/7.1[b]	–	0.6				
		FEP	19.8[a]/1.5[b]	–	0.3				
		PEEK + fluoropolymer	13.4[a]/0.1[b]	–	2				
		Si–O–DLC (PACVD)	29.9[a]/2[b]	–	0.2				
		Ti–DLC (PVD)	41.8[a]/0.4[b]	–	0.2				
Polar component	Low polar component decreases adhesion strength of protein and calcium phosphate	Polished 316 SS	–	–	0.05	Raw whole milk	Batch (60 min) T_{bulk} = 60°C	Distilled water at 25°C (90 s)	Britten et al., 1988
		Standard 316 SS	–	–	0.8				
		PMMA	49.9[a]/19.3[b]	–	0.2				
		PS	43.1[a]/17.1[b]	–	0.1				
		Nylon	67.7[a]/ 19.3[b]	–	2				
		Cellulose acetate	52.6–49.3[a]/29.5–25.1[b]	–	0.2–0.6				
		Agarose coating	72.1[a]/50.5[b]	–	0.3				
	Low polar component reduces fouling amount and calcium phosphate adhesion	2R 316 SS	51.9[a]/39[c]	35.6	–	Simulated milk ultrafiltrate (SMUF)	Batch (5 and 120 min) T_{bulk} = 44°C		Rosmaninho & Melo, 2006
		MoS_2	45.7[a]/20.4[c]	57.8	–				
		SiF^+	49.4[a]/36.8[c]	40.3	–				
		SiO_x	55.5[a]/50.6[c]	18.6	–				
		Ni–P–PTFE	15.5[a]/0.2[c]	118.4	–				
	An optimal polar component leads to decreased fouling resistance and amount	SS	42[a]/8.3[c]	–	0.18	WPI and SMUF SMUF WPI	Batch T_{bulk} = 50 and 40°C for SMUF $T_{surface}$ = 80, 105, 120°C		Boxler et al., 2013
		DLC	45[a]/11.1[c]	–	0.13				
		SICON	46[a]/13.4[c]	–	0.12				

(Continues)

TABLE 3 (Continued)

Investigated parameter	Observations	Coating/Surface	[a]SFE, [b]γ^+, [c]γ^- (mN/m)	WCA (°)	R_a (μm)	Tested fluid	Tested parameters	Rinsing/ cleaning parameters	Reference
		SICAN	46[a]/19[c]	–	0.12				
		SS	42[a]/8.4[c]	–	0.18	WPI and SMUF SMUF WPI	Batch T_{bulk} = 50 and 40°C for SMUF $T_{surface}$ = 80, 105, 120°C	0.25% NaOH solution at 30°C 0.5% NaOH solution at 30°C	Boxler, 2014
		Electropolished SS	46[a]/15.1[c]	–	0.1				
		DLC coating	45.2[a]/13[c]	–	0.13				
		DLC on electropolished SS	47.6[a]/11[c]	–	0.1				
		SICAN	45.2[a]/15.5[c]	–	0.12				
		SICAN on electropolished SS	52.3[a]/14[c]	–	0.11				
		SICON	47.9[a]/22[c]	–	0.12				
		SICON on electropolished SS	55.1[a]/24[c]	–	0.11				
	High polar component decreases fouling amount	2R 316 SS	24.3–39[c]	–	–	SMUF WPI in SMUF	Batch (10 and 120 min) T_{bulk} = 44 and 70°C for SMUF, and 50 and 85°C for WPI in SMUF		Rosmaninho et al., 2008
		MoS_2	50.6–53.8[c]	–	–				
		DLC–Si–O (plasma CVD)	12.4–15.3[c]	–	–				
		SiO_x (plasma CVD)	15–15.6[c]	–	–				
		Ni–P–PTFE	20.4[c]	–	–				
		Silica sol–gel	0.2–10[c]	–	–				
Roughness	Smooth surface leads to lower milk deposit	SS	–	–	0.028	Whole milk	Batch (30 min) T_{bulk} = 90°C		Piepiórka Stepuk et al., 2016
			–	–	0.174				
			–	–	0.445				
Polar component and roughness	High polar component and smooth surface reduce fouling resistance	SS	34[a]/4[b]			WPC in water	Batch (25 h) T_{bulk} = 50°C $T_{surface}$ = 70–80°C	–	Augustin et al., 2007
		Electropolished SS	44[a]/13[b]						
		Aluminium	40[a]/10.5[b]						
		Copper	35[a]/3[b]						
		DLC (PECVD)	45[a]/12[b]						
		SICAN	43.5[a]/6.5[b]						
		SICON	40[a]/19[b]						
		SICAN on electropolished SS	32[a]/3[b]						

Abbreviations: CVD, chemical vapour deposition; DLC, diamond-like carbon; FEP, fluorinated ethylene propylene; PACVD, plasma-assisted CVD; PE, polyethylene; PE HD, polyethylene high density; PECVD, plasma-enhanced CVD; PEEK, polyetheretherketone; PMMA, poly(methyl methacrylate); PP, polypropylene; PTFE, polytetrafluoroethylene; PS, polystyrene; PVD, physical vapour deposition; SICAN, Si-doped DLC; SICON, Si- and O-doped DLC; SMUF, simulated milk ultrafiltrate; SS, stainless steel.

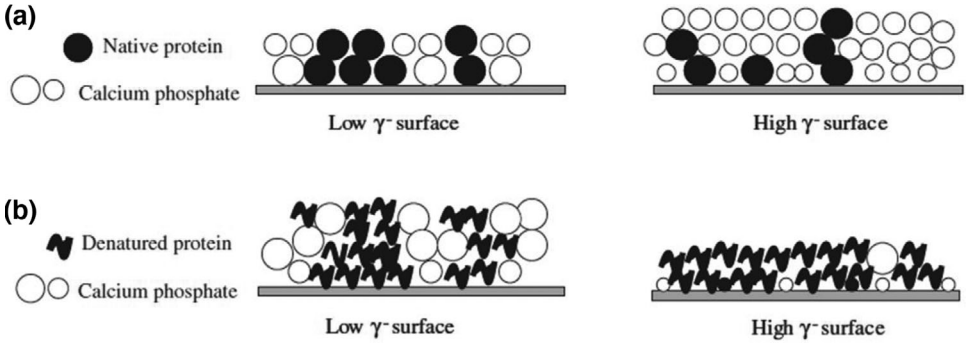

FIGURE 6 Schematic proposed mechanisms of proteins and minerals fouling onto low and high electron donor component surfaces: (a) at low temperature (50°C) and (b) at high temperature (85°C) (Rosmaninho et al., 2008)
Note: Reprinted with permission from Elsevier B.V.

These studies are divided following their observations and conclusions about the influence of surface properties on dairy fouling. Although divergent points of view are ventured, most of them claim that SFE and especially the polar or electron donor components are the main impacting parameters. Kirtley and McGuire (1989) and Mauermann et al. (2009) both investigated protein fouling (β-Lg protein and whey proteins) behavior on various surfaces. Kirtley and McGuire (1989) pointed out that an optimal SFE value is equal to 45.7 mN/m allowing the reduction of β-Lg protein adsorption. On the other hand, Mauermann et al. (2009) did not observe any fouling decrease on modified surfaces (fluoropolymer, diamond-like carbon [DLC] and inorganic coatings). However, coatings with SFE lower than 30 mN/m were easily cleaned. Altogether, no clear correlation between the ease of fouling removal and the SFE or the polar component can be highlighted.

Augustin et al. (2007) also investigated whey proteins fouling on DLC coatings and observed an increase in induction time for higher polar part coatings. However, after 25 hr of pasteurization, the fouling resistance was reduced for coatings having a polar component around 12 mN/m. The latter observation is in agreement with Boxler et al. (2013) who observed a lower mass deposit for surfaces with electron donor (γ^-) component ranging from 8.3 to 13.4 mN/m (2.4 g/mš for Si and O-doped DLC coating compared to 0.6–1.0 g/mš for other coatings) for the same bulk and surface temperatures. As the electron acceptor component of the van Oss model is close to zero, the electron donor component can be compared with the polar part of OWRK model (Augustin et al., 2007; Boxler et al., 2013). In fouling tests, with mineral species only, Rosmaninho and Melo (2008) observed less fouling deposit onto coated surfaces with a low value of the electron donor part as well as for low and high bulk temperatures. This has been refuted by Boxler et al. (2013) and Rosmaninho and Melo (2006) who claimed that a lower fouling resistance for surfaces with higher electron donor component leads to a lower final fouling amount. By investigating raw milk fouling, Britten et al. (1988) demonstrated the impact of a low polar component on the protein and calcium phosphate strength adhesion. Although the fouling amount was comparable on all surfaces, polymeric coatings with a low polar part exhibited lower protein and calcium phosphate adhesion strengths and were easier to clean. Rosmaninho et al. (2008) studied the fouling behavior of whey proteins in presence of minerals at 50 and 85°C, respectively, below and above the denaturation temperature of β-Lg. They observed that at low temperature, the lower the electron donor part, the lower the fouling amount. On the contrary, at high temperature, the higher the electron donor part, the lower the fouling deposit. Consequently, they proposed the mechanisms displayed in Figure 6. At low temperature, the bulk is only composed of native whey proteins and mineral aggregates. These latter are thus able to attach and spread on the surface and preferentially on surfaces of high SFE. On the contrary, at high temperature, denatured whey proteins present in the bulk readily adhere to the surface, hence reducing the adhesion area for minerals attachment.

This high temperature mechanism was confirmed by Boxler et al. (2013) who studied fouling from whey proteins and mineral solution, by heating the surfaces to 85 and 120°C. They observed that calcium phosphate attaches preferentially onto low electron donor component surfaces, and that whey proteins are more abundant onto high electron donor component surfaces. To corroborate their observations, they performed an analysis of variance leading to a decrease of the fouling resistance and fouling mass deposit through an optimal value of the electron donor part.

Piepiórka Stepuk et al. (2016) analysed the fouling behavior of whole milk onto SS with three different roughnesses (R_a: 0.028, 0.174 and 0.445 μm). Contrary to

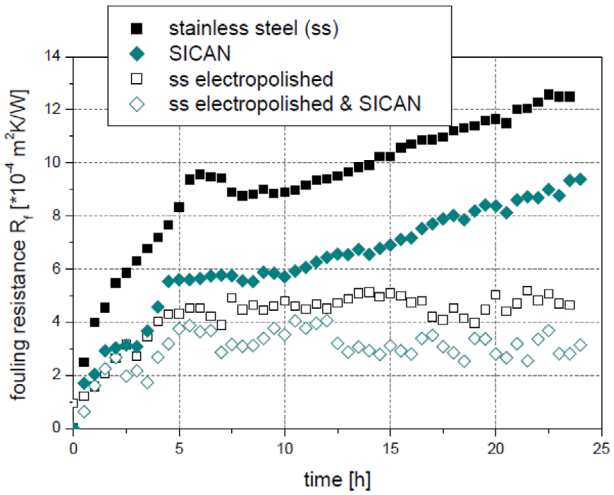

FIGURE 7 Impact of surface roughness and polar component on fouling resistance (Augustin et al., 2007)

previous work, they stated that both the dairy mass deposit and the diameter of deposits were proportional to the surface roughness. They also demonstrated that the smoother the surface, the longer the induction phase.

This confirmed the observations of Augustin et al. (2007), but they pointed out that both the surface roughness and the SFE affect the fouling resistance. Augustin et al. (2007) compared the whey protein fouling resistance of SS with three modified surfaces: Si-doped DLC, electropolished SS and electropolished Si-doped DLC surfaces. The results demonstrated that a high polar component combined with low roughness reduced the fouling resistance as shown in Figure 7.

3.1.2 | Continuous flow pasteurization

The investigations performed under continuous flow conditions are reported in Table 4, in the same way as for batch pasteurization. Among these studies, a few, less than 10, were directly performed in PHEs, as these heat exchangers are widely used in milk pasteurization. Nevertheless, flow rate or flow velocity for these studies remains lower than those used in the dairy pasteurization industrial sector. It can be noted that most of these works were carried out close to or above the denaturation temperature of β-Lg. Therefore, the fouling mechanism is expected to diverge from batch conditions. Whey protein aggregates may form in the bulk and then adsorb on the surface, or the whey proteins may denature on the surface and aggregate. Furthermore, under continuous flow, the average wall shear stress is commonly higher than the one in batch experiments. Thus, fouling is controlled by mass transfer of foulants from the bulk to the heated surface and by erosion of the dairy deposit from the fouling layer back into the bulk. Nevertheless, some studies were carried out with fluid recirculation, which resulted in a decrease in the native β-Lg concentration and an increase in whey protein aggregates in the bulk as the fouling operating time increased. Consequently, the fouling layer consists mainly of denatured and aggregated whey proteins. Without recirculation, milk or model fluid is constantly injected; consequently, at a given position, the composition in fouling species is independent of the time leading to the formation of fouling deposit composed of native, unfolded, denatured and aggregated whey proteins (Boxler, 2014).

Table 4, adapted from Boxler (2014) and Zouaghi (2018), is split into four main topics. Among the published works investigating the influence of surface properties on the dairy fouling behavior, only one claims that SFE and roughness do not affect fouling amount or the cleanability (Patel et al., 2013). Otherwise, it can be noted that the surface properties (SFE, wettability and roughness) of DLC coatings do not differ significantly from the SS surface.

As for batch conditions, SFE and the polar or electron donor component seem to play a greater role than surface roughness on fouling behavior. Santos et al. (2006) analysed whey protein fouling and demonstrated that low SFE coatings lead to a decrease in the amount of whey protein adsorbed, but no direct relationship was established. This observation has been confirmed by Rungraeng et al. (2012), although tests were carried out with pasteurized milk. The nanocomposite carbon nanotubes–polytetrafluoroethylene (PTFE) coating reduces the SFE by 97% compared to bare SS and the final mass fouling by 70%. Liu et al. (2017) demonstrated promising results using ceramic PTFE-free coating having lower SFE than SS, as the fouling deposit was reduced by 98%. Among the surfaces tested by McGuire and Swartzel (1989), PTFE, which has the lowest SFE, does not exhibit the lowest adsorbed mass. McGuire and Swartzel (1989) stated that an optimal SFE value reduces the fouling rate deposition. These observations are at odds with the work of Kananeh et al. (2010) who found no significant fouling reduction using hydrophobic surfaces (PTFE- and polyurethane-based coatings). Nonetheless, these hydrophobic coatings enable to reduce the cleaning time, in particular, PTFE-coated surfaces, which exhibit a drop by 90%. Huo et al. (2019) corroborated the latter observation and demonstrated a 98% improvement in cleaning by modifying SS with a commercial fluoropolymer.

Although different solutions have been used as model fluid for fouling tests, numerous authors pointed out the positive effect of the polar or electron donor component on fouling. Some of them claimed that coatings with low electron donor component reduce the fouling resistance in the first stage as well as decrease the deposition rate and the

TABLE 4 Impact of surface properties on fouling behaviour in continuous flow conditions (adapted from Boxler, 2014; Zouaghi, 2018)

Investigated parameter	Observations	Coating/Surface	[a]SFE, [b]γ^+, [c]γ^- (mN/m)	WCA (°)	R_a (μm)	Tested fluid	Tested parameters	Rinsing/cleaning parameters	Reference
Surface free energy	Low surface free energy resulted in lower absorbed amounts of protein/ in lower mass of fouling	2R 316 SS	–	69	30 nm	Whey protein isolate (WPI) in PBS	Continuous flow, T_{bulk} = 25 and 85°C	–	Santos et al., 2006
		SiF_3^+	–	61	24 nm				
		MoS_2	–	49	25 nm				
		TiC	–	–	20 nm				
		Silica sol–gel	–	–	35 nm				
		DLC (sputtering)	–	84	30 nm				
		DLC (plasma CVD)	–	65	28 nm				
		DLC–Si–O (plasma CVD)	–	–	27 nm				
		316 Stainless steel	32[a]	72.1	–	Pasteurized milk	Continuous flow with recirculation in single channel	–	Rungraeng et al., 2012
		PTFE	5[a]	119.6	–				
		CNT–PTFE	1[a]	141.1	–				
		2B 316L SS	41.4[a]	82.9	0.149	Raw milk	Continuous flow in a benchtop PHE (7 and 5 h) T_{bulk} = 85°C		Liu et al., 2017
		Thermolon sol–gel coating	32.4[a]	105.5	0.199				
	An optimal surface free energy decreases the fouling	Teflon	22.1[a]	–	76	Whole milk	Continuous flow, no recirculation Milk heated from room		McGuire & Swartz, 1989
		Polished 304 SS	46.4[a]	–	1.5				
		Standard 304 SS	51.4[a]	–	16				
		Aluminosilicate coating onto 303 SS	38.6[a]	–	91				
	Low SFE/ hydrophobic coating improves the cleanability	SS	–	83.8	0.15	WPC in water	Continuous flow with recirculation (17 min) T_{bulk} = 45°C $T_{substrate}$ = 96.5°C Continuous flow no recirculation in PHE (4 h) T_{bulk} = 85°C	0.1 molar NaOH solution	Kananeh et al., 2010
		Electrically polished SS	–	61.7/ 60.3	0.17/ 2.69				
		Epoxy resin-based coating	–	97.6/ 91/ 95.8	0.92/ 0.95/ 1.14				
		Polyurethane-based coating	–	93.4	0.06				
		PTFE	–	92.2	0.23				
		304 SS	46.4[a]	–	62.4	WPC in water	Continuous flow (3500 s) T_{bulk} = 60°C	0.5% NaOH solution at 60°C (600 s)	Huo et al., 2019
		Fluorolink S10 coating	19[a]	–	106.7				

(Continues)

TABLE 4 (Continued)

Investigated parameter	Observations	Coating/Surface	[a]SFE, [b]γ^+, [c]γ^- (mN/m)	WCA (°)	R_a (μm)	Tested fluid	Tested parameters	Rinsing/cleaning parameters	Reference
Polar component	Polar component affects fouling resistance and amount	2R 316 SS	39[c]	–	–	WPI in SMUF	Continuous flow, no recirculation (1080–1800 min) T_{bulk} = 48°C	–	Rosmaninho et al., 2007
		TiN 1	55.3[c]	–	–				
		TiN 25	23[c]	–	–				
		TiN 3	46.2[c]	–	–				
	An optimal polar component reduces fouling resistance and amount	SS	43.5[a]/4.6[c]	–	0.17	WPI in SMUF	Continuous flow in PHE T_{bulk} = 62–85°C	–	Boxler et al., 2013
		DLC	47.5[a]/9.2[c]	–	0.21				
		SICON	46.8[a]/13.2[c]	–	0.17				
		SICAN	47.2[a]/8.7[c]	–	0.23				
	Low polar component leads to decreased deposition rate and final amount	2R 316 SS	39[c]	–	–	SMUF	Continuous flow (60 h) T_{bulk} = 48°C	Water at 48°C (48 h)	Rosmaninho et al., 2008
		TiN 1	55.3[c]	–	–				
		TiN 2	23[c]	–	–				
		TiN 3	46.2[c]	–	–				
		TiN 4	18.4[c]	–	–				
		TiN 5	26[c]	–	–				
		304 SS	40.5[a]/8.4[c]	–	0.2	SMUF	Continuous flow with recirculation (900 min) T_{bulk} = 52°C $T_{surface}$ = 50°C	0.5% HNO_3 solution at 52°C	Boxler et al., 2011
		DLC (PECVD)	44.7[a]/13.1[c]	–	0.13				
		Si–DLC (PECVD)	39.4[a]/6.4[c]	–	0.125				
		Si–O–DLC (PECVD)	34.5[a]/7.2[c]	–	0.125				
	Low polar parts tend to reduce mass deposit	2R 304 SS	32.6[c]	57.1	40 nm	Raw milk and WP solution	Continuous flow in microfluidic heat exchanger device (120 min) T_{bulk} = 60–70°C $T_{surface}$ = 105°C Continuous flow with recirculation in bench-scale heat exchanger rig (150 min) T_{bulk} = 60–70°C $T_{surface}$ = 89°C	–	Magens, 2019

(Continues)

TABLE 4 (Continued)

Investigated parameter	Observations	Coating/Surface	[a]SFE, [b]γ^+, [c]γ^- (mN/m)	WCA (°)	R_a (μm)	Tested fluid	Tested parameters	Rinsing/cleaning parameters	Reference
		PP film	0.26[c]	103.5	190 nm				
		PFA-2, PFA-4 (dry powder)	0.53–1.0[c]	110.3/1	617/574 r				
		PFA-3 (water-based suspension)	0.93[c]	108.2	698 nm				
		FEP-2, FEP-3 (water-based suspension)	0.76–1.1[c]	108.4/1	482/269				
		PTFE-2 (water-based suspension)	1.4[c]	106.9	2814 nm				
		PTFE-1 (dispersed in epoxy resin)	11.5[c]	81.1	956 nm				
	Low polar component improves the cleanability	V2 SS	41[a]/14.5[b]	–	0.04	Whole milk with whey protein, sugar, xanthan gum	Continuous flow in PHE, no recirculation $T_{bulk\ outlet} = 102°C$	Water at 60°C (10 min) 0.5 NaOH solution at 60°C (15 min) Water at 60°C (10 min)	Beuf et al., 2003
		DLC	36[a]/9[b]	–	0.1				
		Silica	–	–	–				
		SiO_x	40[a]/13.5[b]	–	0.15				
		Ni–P–PTFE	20.2[a]/5.5[b]	–	0.25				
		Excalibur	21.7[a]/0.9[b]	–	1.77				
		Xylan	21.5[a]/0.95[b]	–	1.81				
		Ion implantation (SiF^+, MoS_2)	45[a]/8[b]/40[a]/12[b]	–	0.2/0.15				
		2B 316L SS	39[a]/3.1[b]	84	0.05	WPI and $CaCl_2$ in water	Continuous flow (1.5 h) $T_{bulk} = 85°C$	Half of samples rinsed with water at 85°C (20 min)	Zouaghi et al., 2018
		Carbonized graphite	48.8[a]/0.6[b]	124.7	0.54				
		PTFE impregnated graphite	49.1[a]/0[b]	116.8	0.27				

(Continues)

TABLE 4 (Continued)

Investigated parameter	Observations	Coating/Surface	[a]SFE, [b]γ^+, [c]γ^- (mN/m)	WCA (°)	R_a (μm)	Tested fluid	Tested parameters	Rinsing/cleaning parameters	Reference
	High polar component could prevent protein adhesion	2B 316L SS	41.9[a]/3.7[b]	84.2	0.068	WPI and $CaCl_2$ in water	Continuous flow (1.5 h) T_{bulk} = 85°C	2% NaOH solution at 85°C (20 min) Water at 85°C (20 min) 2% HNO_3 solution at 85°C (20 min) Water at 85°C (5 min)	Zouaghi et al., 2018
		Si–PEO coating without adhesive layer	51.8[a]/16.7[b]	33.6	0.04				
		Si–PEO coating on plasma activated SS	39.1[a]/9.23[b]	61.6	0.03				
		Si–PEO coating on polydopamine coated SS	50.0[a]/14.1[b]	30.7	0.04				
		Si–PEO coating on NuSil SP120 coated SS	68.8[a]/30.1[b]	28.8	0.02				
Roughness	Micrometric roughness does not reduce fouling or cleanability	Standard 304 SS	–	26	0.13	Raw whole milk	Continuous flow, milk heated in a PHE (72–82 min) T_{bulk} = 86–90°C	Water at 65°C (7 min) 1% NaOH solution at 65°C (14 min) (Only for Teflon)	Yoon & Lund, 1994
		Electropolished SS	–	45	0.08				
		Titanium	–	29	0.19				
		Polysiloxane	–	76	0.1				
		Teflon	–	90	0.6				
	Smooth surface leads to decreased fouling amount	SS	–	–	Pickle finish	Raw milk	Continuous flow with recirculation T_{heat} = 100°C T_{bulk} = 82°C		(Gordon et al., 1968)
			–	–	120 grit finish			–	
			–	–	180 grit finish				
					320 grit finish				
Low surface free energy and smooth surface	Tend to reduce fouling amount	316 SS	41.4[a]	78.8	0.32	Raw milk	Continuous flow in PHE (8 h) T_{bulk} = 85°C	No rinse/low flow water rinse/high flow water rinse/high flow 1 M NaOH rinse	Barish & Goddard, 2013
		Ni–P–PTFE	24.7[a]	115	0.17			Water rinse Half of samples rinsed with water at 85°C (20 min)	

(Continues)

TABLE 4 (Continued)

Investigated parameter	Observations	Coating/Surface	[a]SFE, [b]γ^+, [c]γ^- (mN/m)	WCA (°)	R_a (μm)	Tested fluid	Tested parameters	Rinsing/cleaning parameters	Reference
		2B 316L SS	40.5[a]/3.5[c]	92.9	0.068	WPI and $CaCl_2$ in water	Continuous flow (1.5 h) T_{bulk} = 85°C	Zouaghi et al., 2017	
		Laser-texturised SS	–	0	1243				
		Fluorosilanised laser-texturised SS	–	132.9	1364				
		Slippery surface (fluorine oil Krytox GPL 103)	17.4[a]/3.7[c]	111.6	–				
		2B 316L SS	40.5[a]/3.5[b]	92.9	0.07	WPI and $CaCl_2$ in water	Continuous flow (1.5 h) T_{bulk} = 85°C	–	Zouaghi et al., 2018
		Mirror-like polished SS	42.5[a]/17.0[b]	63.9	0.003				
		Textured SS	–	0	36				
		Fluorosilanized SS	27.6[a]/1.1[b]	111.9	0.98				
		Fluorosilanized mirror-like polished SS	18.8[a]/1.8[b]	105.9	0.004				
		Fluorosilanized textured SS	–	132.9	36				
Polar component and nanostructured surface	Low polar component and nanoroughness lead to reduce fouling amount	2B 316L SS	–	–	105 nm	β-Lg and calcium solution in water	Continuous flow T_{bulk} = 93°C	–	Jimenez et al., 2012
		2B 316L SS (grade 240)	–	–	111 nm				
		2B 316L SS (grade 400)	–	–	68 nm				
		2R 304 SS	–	–	16 nm				
		2B 304 SS	–	–	114 nm				
		TMDSO	0/0.5/0.7[c]	113/112.7/112.8	240/256/280 nm				

(Continues)

TABLE 4 (Continued)

Investigated parameter	Observations	Coating/Surface	[a]SFE, [b]γ^+, [c]γ^- (mN/m)	WCA (°)	R_a (μm)	Tested fluid	Tested parameters	Rinsing/cleaning parameters	Reference
		PTFE–PPS	0.8[c]	116.5	1070 nm				
		Commercial PTFE-based coating	5/6.4/0.3/3.5[c]	87.7/84.3/98.9/88.3	430/451/1055/1064 nm				
	High polar component and nanoroughness decrease final fouling amount	2B 316L SS	41.9[a]/3.7[b]	84.2	0.068	WPI and $CaCl_2$ in water	Continuous flow (1.5 h) T_{bulk} = 85°C	Water at 85°C (20 min)	Zouaghi et al., 2018
		Plasma activated SS	64.7[a]/29.0[b]	23.5	0.07				
		HMDSO coating (APP) PL 1	37.7[a]/3.9[b]	95.7	0.045				
		PL 2	38.4[a]/2.8[b]	79.3	0.051				
		PL 3	44[a]/15.8[b]	101.2	0.043				
		PL 4	46.5[a]/14.5[b]	101.5	0.041				
		PL 5	43.3[a]/7.1[b]	97.1	0.064				
		PL 6	41.5[a]/7.1[b]	94.3	0.049				
		PL 7	48.5[a]/12.7[b]	95	0.04				
		PL 8	42.3[a]/10.2[b]	95.4	0.051				
Surface properties	Do not affect fouling amount or the cleanability	2B 316L SS	50.8[a]/30.2[c]	58.6	0.17	Whole and skim milk and WPI	Batch (120 min) T_{bulk} = 80°C Continuous flow in PHE (240 min) T_{bulk} = 84°C	0.25% NaOH solution at 75°C (10 min) 0.5% HNO_3 solution at 65°C (10 min)	Patel et al., 2013
		Doped DLC 1 (PACVD)	48[a]/21.8[c]	56.6	0.12				
		Doped DLC 2 (PACVD)	43.5[a]/21.2[c]	60.7	0.15				
		Doped DLC 3 (PACVD)	41.3[a]/35.2[c]	50.7	0.13				

Abbreviations: APP, atmospheric pressure plasma; CNT, carbon nanotubes; CVD, chemical vapour deposition; DLC, diamond-like carbon; FEP, fluorinated ethylene propylene; HMDSO, hexamethyldisiloxane; PACVD, plasma-assisted CVD; PECVD, plasma-enhanced CVD; PEO, polyethylene oxide; PFA, perfluoroalkoxy; PHE, plate heat exchanger; PMMA, poly(methyl methacrylate); PP, polypropylene; PPS, polyphenylene sulphide; PTFE, polytetrafluoroethylene; SICAN, Si-doped DLC; SICON, Si- and O-doped DLC; SMUF, simulated milk ultrafiltrate; SS, stainless steel; TMDSO, tetramethyldisiloxane.

TABLE 5 Surface characterizations and fouling density of modified stainless-steel surfaces (adapted from Zouaghi et al., 2018)

Sample	WCA (°)	SFE (mN/m)	R_a (μm)	Density of mass deposit (mg/cmš)
NAT	92.9 ± 4.6	40.5 ± 1.7	0.07 ± 0.01	30.8 ± 4.0
ML	63.9 ± 2.5	42.5 ± 3.8	3.10-3 ± 2.10-4	17.2 ± 0.6
TEX	0 ± 0	Not possible to determine	36.0 ± 2.0	151.2 ± 21.2
SilNAT	111.9 ± 1.1	27.6 ± 3.2	0.98 ± 0.09	8.7 ± 0.6
SilML	105.9 ± 0.8	18.8 ± 4.3	4.10-3 ± 1.10-3	5.2 ± 0.4
SilTEX	132.9 ± 1.6	Not possible to determine	36.0 ± 2.0	57.4 ± 14.3

Abbreviations: NAT, native stainless steel (SS); ML, mirror-like SS; Sil, silanization; TEX, laser-texturized SS.

final fouling amount (Boxler et al., 2011; Magens, 2019; Rosmaninho et al., 2008; Rosmaninho & Melo, 2007). Boxler et al. (2013) demonstrated that a minimal fouling resistance as well as a minimal whey protein adhesion were both obtained for an optimal value of the electron donor component of around 8.5 and 9.5 mN/m. On the other hand, other authors did not observe any reduction in fouling with low polar component surfaces but emphasized the ease of fouling removal after cleaning. Beuf et al. (2003) revealed the cleaning efficiency of Ni–P–PTFE coating and Zouaghi et al. (2018) showed that graphite-based composites led to a fouling drop of 95% after rising with hot water only.

Otherwise, Zouaghi et al. (2018) contradicted all these previous works highlighting that a fouling reduction with a high polar component is also possible. Pasteurization tests were performed using amphiphilic coatings with a high polar component (30.1 mN/m against 3.7 mN/m for SS). No trace of fouling was present after a fouling test, pointing out that high polar part surfaces can also prevent whey protein adhesion.

Based on Table 4, few studies have highlighted the role of surface roughness on dairy fouling as it was noticed for batch pasteurization. In 1968, Gordon et al. (1968) published the first article dealing with the impact of surface modification on dairy fouling. They notably investigated the effect of roughness using SS surfaces with four finishes: pickle finish, which is the roughest, 120 grit finish (R_a: 1.4–2.4 μm), 180 grit finish (R_a: 0.9–1.5 μm) and 320 grit finish (R_a: 0.3–0.5 μm). They concluded that the smoother surface tends to decrease the fouling amount. Yoon and Lund (1994) studied different types of coatings with roughness (R_a) ranging from 0.08 to 0.6 μm. Nevertheless, although this range of surface roughness is lower than that studied by Gordon et al. (1968), no fouling reduction or enhanced cleaning was achieved.

Other authors claimed that mitigation of dairy fouling can only be achieved by taking SFE and roughness into account simultaneously. They pointed out that low SFE combined to a smooth surface leads to fouling mitigation. Zouaghi et al. (2018) investigated the influence of SS surface properties to limit dairy fouling in a holding tube using whey protein and calcium solution. 316L SS 2B finish was considered as the reference (native stainless steel [NAT]), having a SFE of 40.5 mN/m and a R_a of 0.07 μm. Both physical (mirror polishing and laser texturation) and chemical modifications (fluorosilanisation – Sil) were carried out to amplify the roughness or make SS smoother and to reduce the SFE. Surface characterizations as well as fouling densities are gathered in Table 5. It can be noticed that the fouling density of the reference (NAT) is two times greater than the mirror-like SS surface. Furthermore, chemical modification allows to reduce fouling by 83% in the case of fluorosilanized mirror-like SS surface, proving that both SFE and R_a interfere in fouling mitigation.

Barish and Goddard (2013) compared the performance of SS (SFE: 41.4 mN/m and R_a: 0.46 μm) with Ni–P–PTFE coating (SFE: 24.7 mN/m and R_a: 0.17 μm) against raw milk. The density of the fouling mass deposit was significantly lower on the Ni–P–PTFE coating than on the SS surface with 0.45 g/cmš and 12.73 g/cmš, respectively, thus leading to a 96% fouling reduction. Zouaghi et al. (2017) confirmed this observation by using slippery liquid-infused porous surface (SLIPS)-like surfaces. After a pasteurization test, SLIPS-like surfaces allow to limit dairy fouling by up to 63%. Jimenez et al. (2012) corroborate this point of view but emphasise the effect of the electron donor component on fouling mitigation. Comparing samples with equivalent R_a, the lower the electron donor part, the lower the fouling mass. On the contrary, in another work, Zouaghi et al. (2018) deposited silicone-based films onto SS leading to the formation of uneven particles with a R_a ranging from 0.04 to 0.07 μm and with a higher polar component (ranging from 3.92 to 15.8 mN/m) than that of SS surface (3.7 mN/m). These nanostructured surfaces with a high polar part have proved their effectiveness by mitigating dairy fouling by 90%. These works do not allow to establish a correlation between R_a and electron donor component, but a competition can be highlighted.

Finally, comparing impacts of surface properties in batch conditions with those in continuous flow gives similar conclusions. Two points of view can be distinguished: the influence of the electron donor component

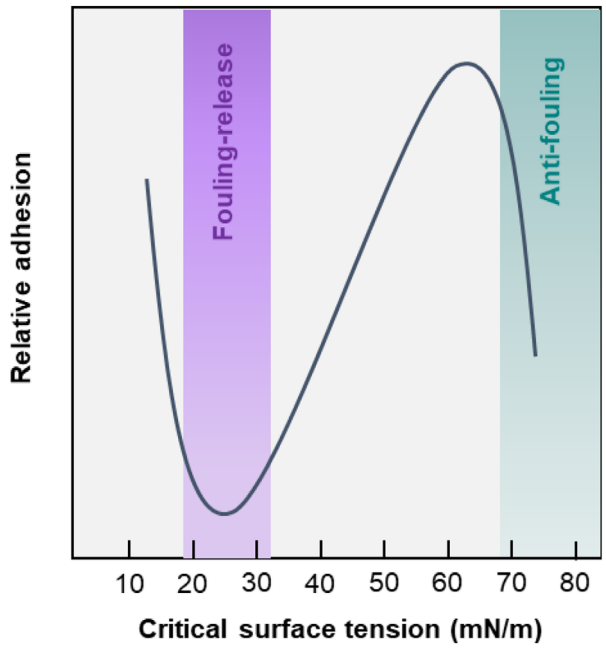

FIGURE 8 Baier's curve of the fouling degree as a function of critical surface tension adapted from (Leonardi & Ober, 2019)

and the combination of the SFE with R_a are discussed in the next sections.

3.1.3 | Impact of SFE

Most studies aimed at reducing the SFE and demonstrating the positive impact of a lower SFE on dairy fouling behavior, whatever the pasteurization type. Overall, SFE acts on the final fouling amount, structure, composition, fouling resistance, deposition rate or cleanability. Nevertheless, a low SFE value does not necessarily enable to minimise the adhesion of proteins onto surface. An optimal SFE range where biological fouling adhesion is minimal has been well established experimentally by Baier (2006), taking place from 20 to 30 mN/m as displayed in Figure 8. This optimal range has been validated for limiting bacteria, mineral and protein adhesion either experimentally or by the Extended Derjaguin–Landau–Verwey–Overbeek (DLVO) theory (McGuire & Swartzel, 1989; Zhao et al., 2004; Zhao et al., 2005; Zhao et al., 2007; Zhao & Müller-Steinhagen, 2001). This range corresponds to fouling-release coatings. The difference between fouling-release and anti-fouling surfaces will be discussed later.

The SFE of SS currently used in dairy industries is around 40 mN/m. Therefore, based on the Baier's relationship (Figure 8), most research attempted to reduce the SFE of SS and thus the polarity. Materials or coatings with low SFE and low polarity are recognized for their anti-adhesive and fouling-release properties, due to weak substrate-fouling deposit adhesions. Two types of materials or coatings are known to fulfil these criteria: silicone and fluorinated materials (Leonardi & Ober, 2019). Both of them have been widely tested against milk or whey proteins and/or calcium solutions.

To limit dairy fouling, silica (Beuf et al., 2003; Rosmaninho et al., 2008; Santos et al., 2006), polysiloxane (Yoon & Lund, 1994) or SiO_x (Beuf et al., 2003; Jimenez et al., 2012; Rosmaninho & Melo, 2006, 2008; Zouaghi et al., 2018) coatings were studied. Albeit, in most cases, SiO_x coatings were deposited by plasma-enhanced chemical vapor deposition (PECVD). Rosmaninho and Melo (2006) and Rosmaninho et al. (2008) obtained coatings with high electron donor component ranging from 15 to 50.6 mN/m unlike Jimenez et al. (2012) who reported more hydrophobic coatings with lower electron donor part ranging from 0 to 0.7 mN/m. Consequently, divergent conclusions were drawn about these coatings. Rosmaninho et al. (2007) did not observe fouling reduction, which was confirmed by Yoon and Lund (1994) with polysiloxane coating, although they also explored the cleanability. On the opposite, Jimenez et al. (2012) and Zouaghi et al. (2018) reported good results in fouling reduction, and after water rinsing as well. But for these latter cases, surface morphology was shown to have a great impact on fouling.

Fluoropolymer materials such as PTFE (Dupeyrat et al., 1987; Gordon et al., 1968; Magens, 2019; Rungraeng et al., 2012; Yoon & Lund, 1994), Ni–P–PTFE (Balasubramanian & Puri, 2008, 2009; Barish & Goddard, 2013; Beuf et al., 2003; Huang & Goddard, 2015; Rosmaninho et al., 2007; Rosmaninho & Melo, 2006; Rosmaninho et al., 2008), fluorinated ethylene propylene (FEP) (Magens, 2019; Mauermann et al., 2009), perfluoroalkoxy alkane (PFA) (Magens, 2019) and commercial coatings (Balasubramanian & Puri, 2008, 2009; Beuf et al., 2003; Huo et al., 2019; Jimenez et al., 2012) have been also investigated. PTFE coating aroused great interest owing to their anti-adhesive properties but its effectiveness is contested. Indeed, Gordon et al. (1968) and Dupeyrat et al. (1987) did not observe a decrease of fouling compared to SS. This was asserted by Yoon and Lund (1994), who investigated the cleanability as well. On the contrary, Rungraeng et al. (2012) demonstrated a 43% fouling decrease compared to unmodified SS. Magens (2019) corroborated this observation; nonetheless, he studied other fluoropolymer coatings and showed that PFA and FEP were more efficient. This could be explained by the combination of their low SFE with their low R_a compared to PTFE coatings. Unlike PTFE coating, Ni–P–PTFE coating presents higher performance to mitigate dairy fouling and is also easier to clean. Most authors pointed out a synergy between a lower electron donor component and a smooth surface masking grain boundaries of SS (Barish & Goddard, 2013; Beuf et al., 2003).

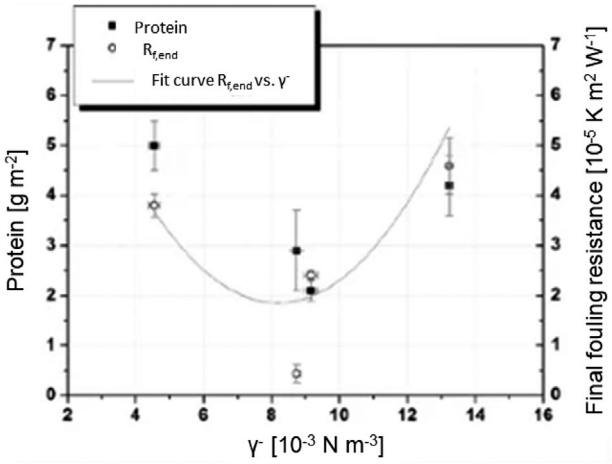

FIGURE 9 Analysis of the influence of the electron donor component on deposit protein content and final fouling resistance (Boxler et al., 2013)

Divergent conclusions for PTFE or SiO_x coating can be explained by the fact that the adhesion of hydrophilic molecules such as proteins is favourable on low-energy surfaces, but larger conformational changes of β-Lg were observed on hydrophobic than on hydrophilic surfaces (Karlsson et al., 1996). Moreover, the presence of Ca^{2+} reinforces protein adhesion acting as electron acceptor, neutralising electron donor sites on surface, thus the surface becomes more hydrophobic (van Oss, 2006). Some authors have therefore tried to correlate the electron donor part to fouling behavior. Britten et al. (1988) found that the polar component is the main parameter affecting the strength adhesion of proteins. The bacteria adhesion was correlated with the ratio of the Lifshitz–van der Waals (γ^{LW}) part over the electron donor (γ^-) part. This was confirmed by Boxler et al. (2013) who found an optimal electron donor component around 8.5–9.5 mN/m (Figure 9). Rosmaninho et al. (2008) and Liu et al. (2011) also found optimal electron donor values affecting fouling, but much larger, ranging from 10 to 55 mN/m.

3.1.4 | Impact of roughness

As mentioned in Section 2, R_a is related to SFE through wettability. Therefore, very few works have analysed the effect of R_a on dairy fouling alone because it is complex to isolate. Gordon et al. (1968) investigated SS surfaces with different R_a and concluded that the lower the R_a, the lower the dairy deposit. This observation was further validated by Piepiórka et al. (2016) and Zouaghi et al. (2018) who have also explored roughness of SS surfaces. Piepiórka et al. (2016) emphasized that R_a affects the fouling structure as well. They found larger clusters on surfaces with higher R_a. By comparing SS to electropolished SS, Boxler (2014) observed a lower fouling resistance on the electropolished one. Moreover, the structure of electropolished SS differs from that of SS. Boxler (2014) assumes that smoother surfaces are more prone to the adhesion of aggregated whey proteins and mineral agglomerates than rough surfaces hinge on the large diameter of whey proteins and mineral aggregates, ranging from 5 to 100 μm (Ndoye et al., 2013; Petit et al., 2013; Zúñiga et al., 2010) and 0.1 to 80 μm (Dey et al., 2010; Rosmaninho et al., 2003), respectively. Hence, aggregated whey proteins and mineral agglomerates must diffuse into the boundary grains before being adsorbed. On the contrary, rough surfaces favour prevail the attachment of native (1–10 nm; Boxler, 2014) and denatured whey proteins (50–60 nm; Jimenez et al., 2013) as well as calcium and phosphate clusters (1 nm; Boxler, 2014), as depicted in Figure 10. Jimenez et al. (2012) confirmed the latter hypothesis by observing calcium deposit at the grain boundary, leading to an increase in dairy fouling.

Surface morphology affects the structure and fouling deposit amount but also the cleanability. According to Detry et al. (2010), fouling can remain into surface defects even after cleaning. Reducing R_a could thus facilitate fouling removal. However, Yoon and Lund (1994) studied several substrates with roughness ranging from 0.08 to 0.6 μm and claimed that R_a difference had no impact on fouling amount or on cleanability. Given the size of proteins and minerals depending on their state, R_a was, however, too high to prevent fouling adhesion. This has been proved by Zouaghi et al. (2018) who reported that nano-rough surfaces (< 0.05 μm) enable the reduction of fouling after water rinsing.

Although, according to these investigations, a low R_a leads to milk fouling reduction and easier cleaning, to date no correlation has been established. Nevertheless, several authors stated that both low SFE and R_a at the nanoscale lead to a decrease of fouling deposit and improve the cleaning step. Zouaghi et al. (2018) demonstrated that, by lowering both SFE and R_a, fouling was reduced by 83%. Barish and Goddard (2013), Zouaghi et al (2017) and Jimenez et al. (2012) validated this conclusion, suggesting a competition between both surface parameters for fouling control.

3.2 | Design of surfaces mitigating dairy fouling

The design of materials or coatings mitigating dairy fouling was developed in the 1990s with the outbreak of new high-performance technologies for producing nanomaterials. The latter are elaborated following two different approaches gathering several manufacturing

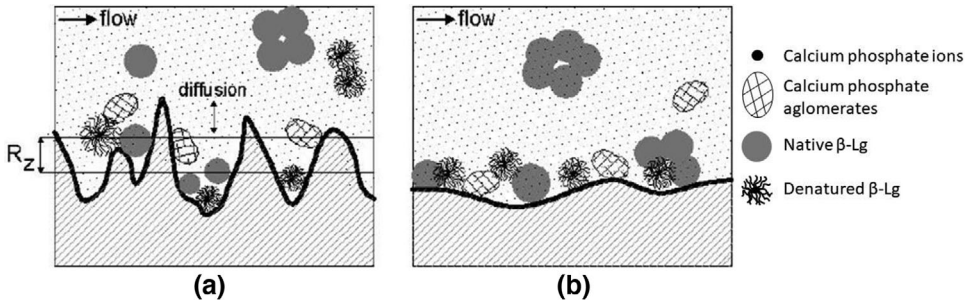

FIGURE 10 Impact of roughness depth (R_z) on the formation of the first fouling layer from a solution of whey proteins and calcium phosphates: (a) onto unpolished stainless-steel surface and (b) onto electropolished stainless steel surface (Boxler, 2014)

TABLE 6 Top-down techniques

Fabrication method	Type of coating	Industrialisable method	References
Electropolishing	Electropolished stainless steel	✓	Augustin et al., 2007; Boxler, 2014; Kananeh et al., 2010; Yoon & Lund, 1994
Chemical etching	Pickling process for Ni–P–PTFE coating	✓	Barish & Goddard, 2013; Beuf et al., 2003; Rosmaninho & Melo, 2006
Laser etching	Surface structuration for Slippery liquid-infused surface	✗	Zouaghi et al., 2017

processes. The first one is the top-down method, where matter is removed from the material to give a structured surface, whereas the bottom-up method consists matter deposition to build-up the wanted surface. As for nanomaterials, processes used to design surfaces for reducing dairy fouling have been divided into two groups.

3.2.1 | Top-down techniques

The top-down approach consists sculpting a raw material (from the top) in order to obtain new micro- or nanostructures (down) with new properties (physical or chemical). Micro-nanofabrication processes by etching/ablating-based methods (dry or wet etching) allow creating micro- or nano-roughness on smooth surfaces to structure a material. When combined to a lithography process or other masking methods, a periodic or quasi-periodic network can be obtained.

The top-down techniques used to design surfaces limiting dairy deposit are gathered in Table 6. Electropolishing process was used either alone to decrease intrinsic roughness of SS or combined with a bottom-up technique (see next section). Most of top-down processes displayed, such as chemical or laser etching, providing specific roughness to SS, have been combined with a bottom-up procedure leading to Ni–P–PTFE or SLIPS-like coatings for example. Procedures of fabrication of both of these coatings will be described later. Globally, techniques gathered in Table 6 are used either to decrease or to increase intrinsic roughness of SS. Recently, Ahn et al. (2019) have used electrochemical etching to make porous SS PHEs with holes at the micro and nano scale. However, these modified surfaces were tested against an inorganic fouling, $CaCO_3$, closer to type B fouling (mineral fouling).

3.2.2 | Bottom-up techniques

The bottom-up approach refers to an assembly of small building blocks (molecules/atoms) (bottom) to form larger and more complex object (up) with new properties. The fabrication methods mainly require physical and chemical-based processes. Bottom-up processes have been much more investigated than top-down techniques in the dairy industry. Indeed, as shown previously, surface modifications have been performed in order to reduce the SFE of SS. This has been achieved, in most cases, by depositing coatings directly on SS surfaces and thus using only bottom-up techniques. These latter are reported in Table 7.

These techniques of fabrication can be also divided in two categories: (i) the wet route and (ii) the dry route. Wet routes gather sol–gel, self-assembly and electroless deposition methods, whereas dry routes gather ion implantation, physical vapor deposition, sputtering, chemical vapor deposition (CVD), plasma-assisted chemical vapor

TABLE 7 Bottom-up techniques

Fabrication method	Type of coating	Industrialisable method	References
Sol–gel	Inorganic and hybrid nanocomposites	✓	Mauermann et al., 2009
	Silica		Beuf et al., 2003; Santos et al., 2006
	Thermolon		Liu et al., 2017
Self-assembly	Silanization step for Slippery liquid-infused surface	✓	Zouaghi et al., 2017
Casting solution	PMMA, PS, cellulose, agarose and nylon	✓	Britten et al., 1988
	Amphiphilic Si–PEO		Zouaghi et al., 2018
Electroless deposition	Ni–P–PTFE	✓	Barish & Goddard, 2013; Beuf et al., 2003; Rosmaninho & Melo, 2006
Ionic implantation	SiF_3^+	✗	Rosmaninho & Melo, 2006; Santos et al., 2006
	SiF^+		Beuf et al., 2003
	MoS_2		Beuf et al., 2003; Rosmaninho & Melo, 2006; Santos et al., 2006
	TiC		Santos et al., 2006
PVD	Ti–DLC	✗	Mauermann et al., 2009
	TiN		Rosmaninho et al., 2007, 2008
	DLC		Santos et al., 2006
CVD	DLC	✗	Santos et al., 2006
	Si–O–DLC		Santos et al., 2006
	Multiwalled carbon nanotubes for CNT–PTFE coating		Rungraeng et al., 2012
PACVD	Si–DLC	✗	Mauermann et al., 2009
	Doped DLC		Patel et al., 2013
PECVD	DLC	✗	Augustin et al., 2007; Beuf et al., 2003; Boxler et al., 2011, 2013a, 2013b
	Si–DLC		Boxler et al., 2011
	Si–O–DLC		Boxler et al., 2011
	SICAN		Augustin et al., 2007; Boxler et al., 2013a, 2013b
	SICON		Augustin et al., 2007; Boxler et al., 2013a, 2013b
	SiO_x		Beuf et al., 2003; Rosmaninho & Melo, 2006; Rosmaninho et al., 2008
	TMDSO		Jimenez et al., 2012
APP	HMDSO	✓	Zouaghi et al., 2018

Abbreviations: APP, atmospheric pressure plasma; CNT, carbon nanotubes; CVD, chemical vapour deposition; DLC, diamond-like carbon; HMDSO, hexamethyldisiloxane; PACVD, plasma-assisted CVD; PECVD, plasma-enhanced CVD; PEO, polyethylene oxide; PMMA, poly(methyl methacrylate); PTFE, polytetrafluoroethylene; PVD, physical vapour deposition; SICAN, Si-doped DLC; SICON, Si- and O-doped DLC; TMDSO, tetramethyldisiloxane.

deposition, PECVD and atmospheric pressure plasma (APP). As displayed in Table 7, most of coatings are produced by dry routes. These procedures are more environmentally friendly than wet routes as they do not require the use of solvents or catalyst, but require specific equipment. DLC, silicon-based and implanted ion coatings have been amply elaborated by these dry routes.

DLC coatings have been extensively produced through various dry methods due to their numerous attractive properties (Augustin et al., 2007; Beuf et al., 2003; Boxler et al., 2011, 2013a, 2013b; Mauermann et al., 2009; Santos et al., 2006). DLC coatings demonstrate good thermal conductivity, similar to that of metals, and are extremely smooth, wear resistant and hard (Grill, 1993; Robertson, 2002). In addition, the amorphous nature of DLC coatings allows their mechanical properties and surface free energies to be adjusted by introducing specific elements. The incorporation of Si or F in the DLC matrix results in the decrease of SFE. The opposite tendency is observed by adding O or N in the matrix (Donnet, 1998; Trojan et al., 1994). As reported

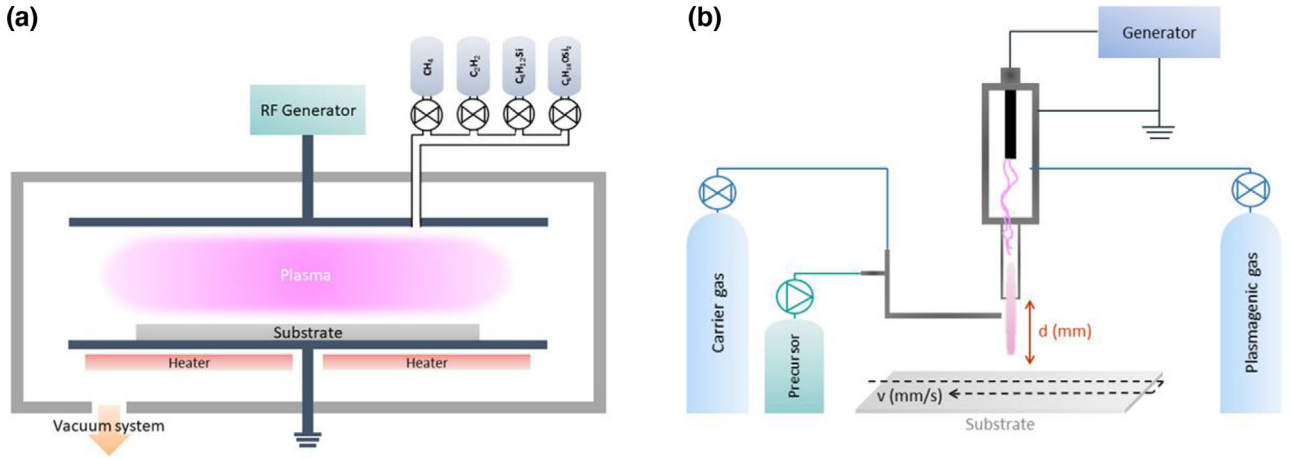

FIGURE 11 (a) Plasma-enhanced chemical vapour deposition (PECVD) technique, (b) atmospheric pressure plasma (APP) torch

in Table 7, DLC and doped DLC have been produced by various vacuum deposition methods, and PECVD is the most used (Figure 11). As CVD process, PECVD method enables to growth thin films onto a substrate through gaseous phase. Here, plasma is usually generated through radio frequency radiations or microwaves, allowing chemical reactions of gaseous precursors injected in the vacuum chamber. Properties and growth of thin films can be controlled via several parameters such as gas pressure, gas nature, power and substrate temperature. Various gases are used to grow DLC films. C_xH_x gases such as methane or acetylene are typically chosen as carbon sources to obtain DLC coatings, whereas tetramethylsilane, hexamethyldisiloxane (HMDSO) or tetrafluorethylene are Si and F sources, respectively, allowing the formation of doped DLC coatings.

As explained above, silicon-based coatings were widely investigated due to their numerous properties (chemically stable and inert, environmentally friendly, smooth surface, drag reduction) (Hu et al., 2020) and have demonstrated interesting results either to reduce dairy deposit or facilitate fouling removal. Silica and SiO_x coatings were prepared from organosilicon precursors such as methyltriethoxysilane, tetramethydisiloxane and HMDSO. These molecules have been widely used to deposit hydrophilic SiO_x coatings as adhesive or gas barrier film. Santos et al. (2004), Rosmaninho and Melo (2006) and Rosmaninho et al. (2008) obtained hydrophilic silicon-based coatings elaborated either by sol–gel or PECVD processes. However, other authors have proven that hydrophobic coatings could be obtained using PECVD or APP processes (Beuf et al., 2003; Jimenez et al., 2012; Zouaghi et al., 2018). By optimising manufacturing parameters of these dry methods, silicon-like coatings can be obtained. Under plasma discharge, such organosilicon monomers form a strong –Si–O–Si– backbone with terminal CH_x functions conferring hydrophobic properties. Although repeatable and reliable, PECVD processes are time-consuming and expensive due to the use of vacuum pumps and chambers. To scale up plasma treatments for industrial applications, APP sources have been developed. Zouaghi et al. (2018) deposited silicon-based coatings using an APP torch (Figure 11), commercialized by AcXys Technologies, and they obtained hydrophobic coatings by injecting HMDSO as precursor in the plasma post-discharge. According to Dimitrakellis and Gogolides (2018), HMDSO is largely chosen to form hydrophobic coating by APP hinge on its chemical inertness, high vapour pressure and low toxicity.

Some authors have also used ionic implantation to modify SS surface. This process consists implanting atoms on the surface of a solid substrate. Ions are accelerated in the keV to MeV energy range and then hit the surface to slot into the uppermost layers of the surface (Mayer et al., 1970). Depending on the accelerating energy of ions, their mass, and the mass of the atoms of the targeted material, ions can penetrate to a depth from 10 to 1000 nm. Therefore, ion implantation can change SFE and R_a without changing the bulk properties. Based on the Electric Double Layer theory, Zhao and Burnside (1994) stated that both the free electrons on the metal surface and the SFE can be reduced by implanting elements having less free electron than pure metal (F, Si, C, …) (Dhillon, 2012; Müller-Steinhagen & Zhao, 1997). This technique allows doping the surface, thus no adhesion issues such as in CVD are observed. Two types of ion implantation have been used to reduce the SFE of SS: (i) direct ion implantation, which is described above, and (ii) turbulent ion implantation (Figure 12). The latter technique is comparable to sputtering where the substrate is directly in contact with a plasma, but in this case, the substrate is placed at the cathode. Due to collisions in the plasma, atoms can penetrate the surface deeper, up to 100 μm. MoS_2 particles were injected in the vacuum

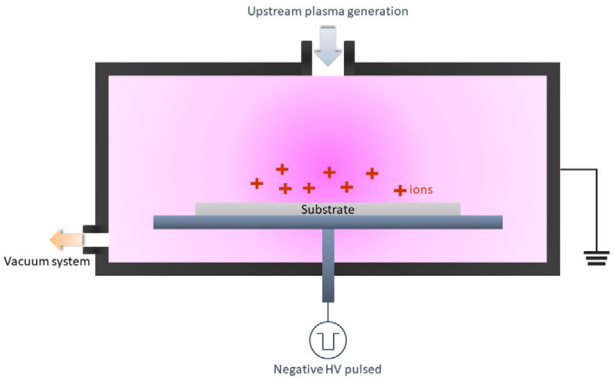

FIGURE 12 Schematic diagram of turbulent ion implantation process

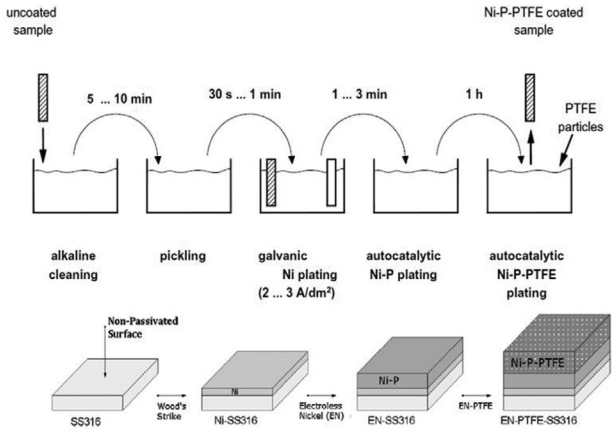

FIGURE 13 Process of fabrication of Ni–P–PTFE coating (Barish & Goddard, 2013; Santos et al., 2004)
Note: Reprinted with permission from Elsevier B.V.

chamber in order to be implanted into the SS surface, as it is used as anti-adhesive in the mechanical engineering field (Beuf et al., 2003; Santos et al., 2004). Nevertheless, XPS analyses exhibited a very low content of implanted molybdenum compared to bare SS due to the low concentration of MoS_2 particles used in the process.

3.2.3 | Combination of top-down and bottom-up approaches

Some of the studies cited above report combination of top-down and bottom-up approaches: Ni–P–PTFE coatings and SLIPS-like surfaces. These were elaborated following different steps. The fabrication of Ni–P–PTFE coatings was reported by Santos et al. (2004) and Barish and Goddard (2013) and SLIPS-likes surfaces were detailed by Zouaghi et al. (2017).

The process of fabrication of Ni–P–PTFE coatings is illustrated in Figure 13. First, the SS substrate is submitted to a pickling process consisting of preparing the surface by removing impurities and/or oxide layer. Then, the activated substrate undergoes a galvanic deposition of Ni followed by an autocatalytic reaction depositing a Ni–P plating. Finally, nanoparticles of PTFE are incorporated in the Ni–P matrix.

Numerous ways exist to design SLIPS, which have been reviewed by Howell et al. (2018) recently. Zouaghi et al. (2017) developed their own SLIPS-like surfaces in order to mitigate dairy fouling. The first step was to roughen the SS using femtosecond laser ablation. Cauliflower-like surfaces were obtained and the roughness raised from 68 to 1243 nm, as shown in Figure 14. After that, these surfaces were activated using a UV/ozone cleaner generating hydroxyl groups. These surfaces were then silanized with a perfluorosilane, prior to being impregnated by a perfluorinated oil (DuPont Krytox GPL 103).

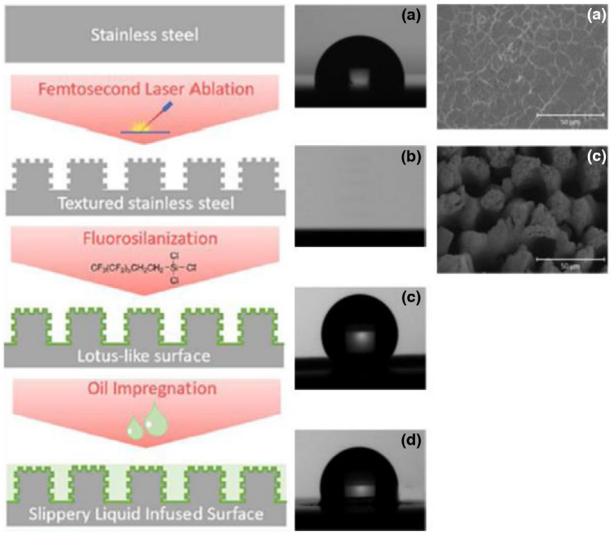

FIGURE 14 Elaboration of SLIPS-like surface with the wettability corresponding to each step of fabrication and the surface morphology of stainless steel before and after the laser ablation (Zouaghi et al., 2017)
Note: Reprinted with permission from American Chemical Society.

4 | ANTI-FOULING AND FOULING-RELEASE SURFACES

4.1 | Anti-fouling or fouling-release surfaces

In dairy fouling field, the distinction between anti-fouling and fouling-release surfaces is not always evident. According to Leonardi and Ober (2019) and Hu et al. (2020), anti-fouling surfaces prevent the attachment of proteins, bacteria and microorganisms as displayed in Figure 15 (Hu et al.,

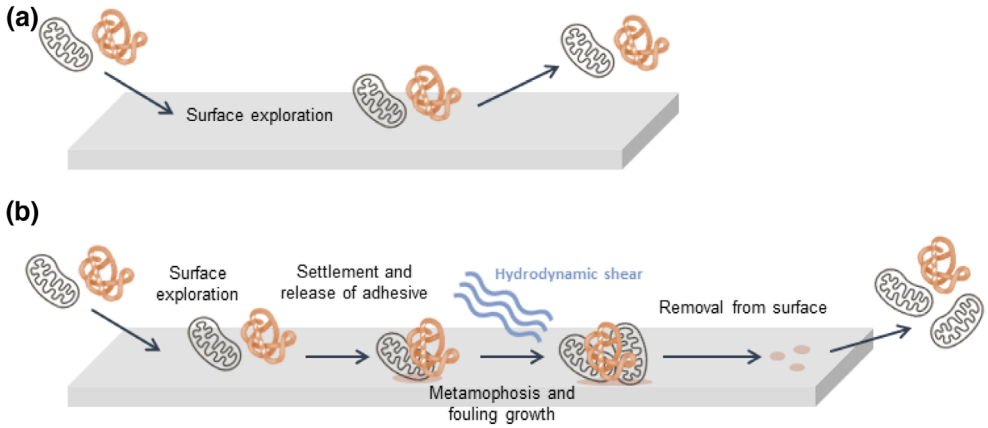

FIGURE 15 Schematic mechanisms of (a) anti-fouling surfaces and (b) fouling-release surfaces (adapted from Leonardi & Ober, 2019)

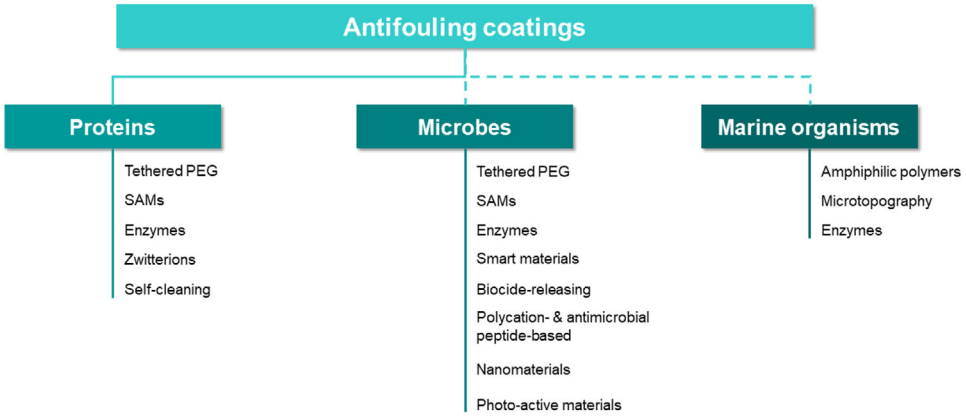

FIGURE 16 Ways of designing anti-fouling surfaces (adapted from Banerjee et al., 2011)

2020; Leonardi & Ober, 2019). Contrary to anti-fouling surfaces, fouling-release surfaces allow the ease removal of bacteria, proteins or microorganisms through hydrodynamic shear stress coming from mechanical cleaning or the ships' navigation in marine field (Figure 15). Based on these definitions, this section will distinguish anti-fouling surfaces from fouling-release surfaces conceived for dairy fouling mitigation.

4.2 | Anti-fouling surfaces

Banerjee et al. have reviewed the different ways for designing anti-fouling coatings preventing adsorption of proteins, bacteria and marine organisms. Various solutions are reported as displayed in Figure 16. Most of them have been extensively explored in biomedical and marine fields. Banerjee et al. (2011) subdivided coatings preventing proteins adhesion in two categories: (i) resistant coating and (ii) degrading coating. Coatings resisting to protein adhesion gather tethered PEG (polyethylene glycol), self-assembled monolayers (SAMs) and zwitterions, whereas coatings degrading protein correspond to enzymes and self-cleaning surfaces.

According to the literature, only one of these techniques has been used against β-Lg. Wei et al. (2003) investigated SS modified by a PEG layer aiming at hindering protein adsorption. Due to the poor adhesion of PEG onto SS, the surface was first functionalized with amine groups. Polyethylenimine (PEI) was physisorbed onto SS surface, allowing PEG grafting through amine groups. These PEG surfaces were then immersed in a β-Lg solution at room temperature for 1 hr. Wei et al. (2003) pointed out that the higher the concentration of PEI, the higher the grafted PEG amount. Surfaces were analysed before and after immersion by ToF-SIMS. As shown in Figure 17, no difference of intensity was observed for SS–PEI(30)–PEG before and after immersion. Hence, β-Lg protein adsorption was prevented for the highest PEI concentration.

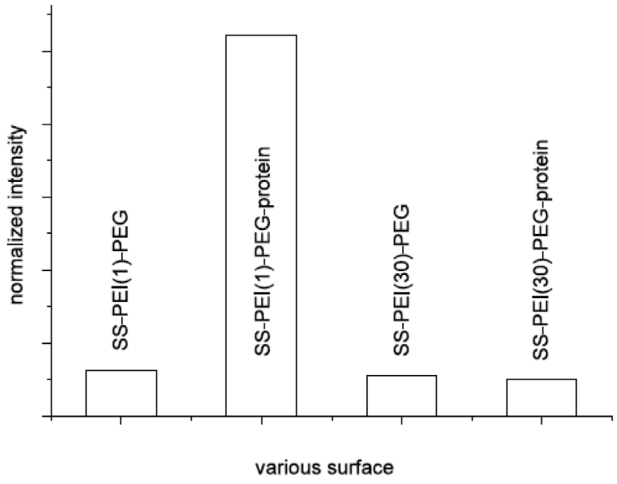

FIGURE 17 Anti-fouling performances of SS–PEI–PEG surfaces as a function of grafted PEG amount (Wei et al., 2003)
Note: Reprinted with permission from Elsevier B.V.

Albeit these results exhibit promising anti-fouling performance to reduce β-Lg protein adsorption, the adhesion tests were performed at room temperature, well below the denaturation temperature and under static mode. These conditions are not representative of a pasteurization cycle. Thus, it is intricate to conclude on the effectiveness of these PEG coatings for mitigating dairy fouling as well as on their advantages and drawbacks.

To date, other types of anti-fouling coatings were not assessed in the mitigation of dairy fouling. Although they proved their effectiveness in biomedical or marine field, they present drawbacks that could limit their action for preventing dairy deposits. Protein-resistant coatings based on SAMs with oligo(ethylene glycol) terminations display higher anti-fouling performance than tethered PEG surfaces and are easy to fabricate but they are less robust due to the presence of defects (Hucknall et al., 2009; Ma et al., 2004). It could lead to a loss of anti-fouling performance at high flow rate. According to Leonardi and Ober (2019), zwitterions are a promising alternative to PEG coatings in the marine sector; however, the elaboration of zwitterionic surfaces is troublesome. Monomers are often expensive, their dissolution in organic solvent remains complex and they are unstable during polymerisation reactions (Laschewsky, 2014). Among coatings degrading proteins, enzyme-based surfaces seem unfavourable to mitigate dairy fouling. Enzymes are proteins with a catalytic activity. Thus, as whey proteins, enzymes are mostly thermosensitive. Indeed, when they are submitted to high temperature, they denature, leading to a loss of activity. Protein adhesion tests performed on enzyme-based surfaces are usually carried out between 30 and 40°C (Asuri et al., 2007; Kim et al., 2001). The last type of surface reported by Banerjee et al. (2011) is photoactivated self-cleaning coating, where foulants are decomposed by ultraviolet or visible radiation (Banerjee et al., 2011). TiO_2 particles are commonly used as photocatalyst for that purpose. Nonetheless, once again, transfer of photoactivated coating to dairy field is objectionable, knowing that TiO_2 is recognized for being potentially carcinogenic to humans. Hence, the use of TiO_2 particles could cause health issues if they get entrapped in dairy products (Jovanović, 2015).

4.3 | Fouling-release surfaces

As previously noticed, based on Baier's relationship between the SFE and foulants' adhesion, research was widely focused on surface modification of SS in order to reduce its SFE. Moreover, due to the weaker adhesion of foulants combined with hydrodynamic shear stress, fouling-release surfaces are easier to clean. Thus, in the literature, some works have investigated the cleanability of different materials and coatings. However, it is intricate to compare the cleaning effectiveness of coatings with each other. Indeed, as displayed in Tables 3 and 4, numerous cleaning conditions were used in both batch and continuous flow conditions. Some of them have chosen harsh conditions, close to those used in CIP procedures, and others have assessed fouling-release performances with water only.

A recent study has investigated the influence on the wetting behavior of different concentrated cleaning solutions (NaOH) and water on the surface foulant as the function of the surface temperature. In food industries, CIPs are now standard automated techniques, avoiding the dismantlement of processing equipment. The circulation of cleaning solutions aims at re-establishing the initial pressure and heat transfer performances and at countering microbial risks contamination through surface disinfection. CIP procedures can be detailed in five steps: (i) pre-rinsing, (ii) detergent cycle, (iii) intermediate rinsing, (iv) sanitization, and (v) final rinsing (Fryer & Christian, 2005). The second cleaning step 'detergent cycle' can be completed in a single-stage process (with the use of acidic or alkaline solutions or detergents) or in a two-stage process (Timperley & Smeulders, 1987).

An example of a two-stage process has been detailed by Bylund (1995) as follows. First, processing equipment is pre-rinsed with hot water for about 10 min to remove excess, weakly adhering, fouling deposits from the surface. Then, heat exchanger surfaces undergo a chemical cleaning to release the fouling deposit with (i) an alkaline solution (0.5%–1.5%) at 75°C for 30 min removing organic foulants such as proteins, (ii) warm water for 5 min for rinsing out alkaline solution (NaOH) and (iii) an acidic

TABLE 8 Classification of cleaning conditions

Cleaning conditions		References
Green cleaning	Water	Barish & Goddard, 2013; Britten et al., 1988; Rosmaninho et al., 2008; Zouaghi et al., 2018; Zouaghi et al., 2018
Soft cleaning	≤0.5% NaOH solution and ≤0.5% HNO_3 solution	Beuf et al., 2003; Boxler, 2014; Boxler et al., 2011; Huo et al., 2019; Premathilaka et al., 2006, 2007; Rosmaninho et al., 2007
Harsh cleaning	≥1% NaOH solution and ≥0.5% HNO_3 solution	Barish & Goddard, 2013; Kananeh et al., 2010; Mauermann et al., 2009; Yoon & Lund, 1994

solution (HNO_3, H_3PO_4) (0.5%–1%) at 70°C for 20 min to eliminate inorganic components such as mineral species. This is followed by a post-rinsing with cold water to remove all traces of fouling deposits and chemical cleaning (chlorinated agents) from the system, subsequent surface disinfection and a final water rinse.

Fouling-release surfaces can present real advantages concerning environmental and economic costs of cleaning in dairy thermal processing. Most of chemical solutions are not biodegradable, dairy wastewaters have to undergo several post-treatments and dairy thermal treatments processes are regularly shut down to be cleaned.

An investigation (Magens et al., 2016) pointed out that an optimal cleaning time could increase the cost-effectiveness of modified surfaces. Using modified SS surfaces would allow the cleaning to be spaced from 24 to 100 days. This would reduce cleaning cost up to 35%. To go further, in a life cycle assessment study, Zouaghi et al. (2019) demonstrated that repeated CIP burdens the environmental footprint of the pasteurization process. They pointed out that surface modification leading to clean surfaces with water only (no need of detergents) reduces the environmental impact of the pasteurization process by more than 70%.

Zouaghi et al. (2018, 2018) presented works with drastic reduction of fouling after water rinsing only. Works having investigated the cleaning behavior are gathered in Table 8 and are classified as a function of the cleaning conditions in three categories: (i) green cleaning, (ii) soft cleaning, and (iii) harsh cleaning.

Overall, most of the studies having investigated the cleanability agreed that surfaces with low SFE and more precisely low polar component are easier to clean. Consequently, surfaces with a low polar component demonstrate good fouling-release properties. Nevertheless, it is clear that materials or coatings cleaned only with water are extremely promising. Therefore, we will focus on these surfaces.

Britten et al. (1988) did not directly investigate the cleanability but they analysed the strength of adhesion of dairy deposit onto surfaces. They stated that the strength of adhesion is the key parameter determining the work of adhesion between the surface and the deposits such as proteins or minerals. The work of adhesion (W_A) is defined as the required energy to separate the liquid phase from the solid one and is related to the SFE of the solid (γ_{SV}) and liquid (γ_{LV}) and the interfacial tension between the liquid and the solid (γ_{SL}) as follows (Dupeyrat et al., 1987):

$$W_A = \gamma_{SV} + \gamma_{LV} - \gamma_{SL}. \quad (7)$$

Consequently, the lower the SFE, the weaker the adhesion between the surface and proteins and minerals, hence increasing the ease of removal. Here, the strength of adhesion was analysed using an ultrasonic bath in distilled water at room temperature for 300 s inducing shear stress. After that, bare SS surface was still fouled, whereas all coated surfaces were almost cleaned (Britten et al., 1988). In that case, no conclusion can be drawn on the efficiency of water rinsing under shear stress. Indeed, the proportion of fouling deposit removal is not evaluated for SS surface or coated surfaces. This could have been carried out by weighing surfaces before and after water rinsing. Hence, it is hard to conclude what is the most promising fouling-release coating among the polymer coatings tested.

In order to remove both loose and harder adsorbed fouling deposit, Rosmaninho et al. (2008) analysed cleaning performances of 2R SS and TiN surfaces in two stages. The first cleaning step was performed at the same flow velocity than the fouling experiment and the second one at higher flow velocity, both in water at 48°C for 24 hr. The second cleaning stage was more effective. Nevertheless, despite that TiN surfaces were less fouled than 2R SS surface, important fouling amount still remained on both surfaces (Rosmaninho et al., 2008). Barish and Goddard (2013) compared the cleanability of unmodified SS surface and Ni–P–PTFE-coated one through three cleaning conditions: (i) deionized water at same flow rate of fouling experiment, (ii) deionized water at higher flow rate, and (iii) NaOH solution (1 M) at higher flow rate. Although the increase of water flow rate led to a reduced fouling amount for both surfaces (13% for SS and 36% for Ni–P–PTFE), alkaline cleaning led to a drastic drop of dairy deposit, reaching 78% and 93% for SS and Ni–P–PTFE coating, respectively. As concluded by Rosmaninho et al. (2008), water rinsing does not provide satisfying results; however, cleaning time and temperature were not indicated in this study. Zouaghi et al.

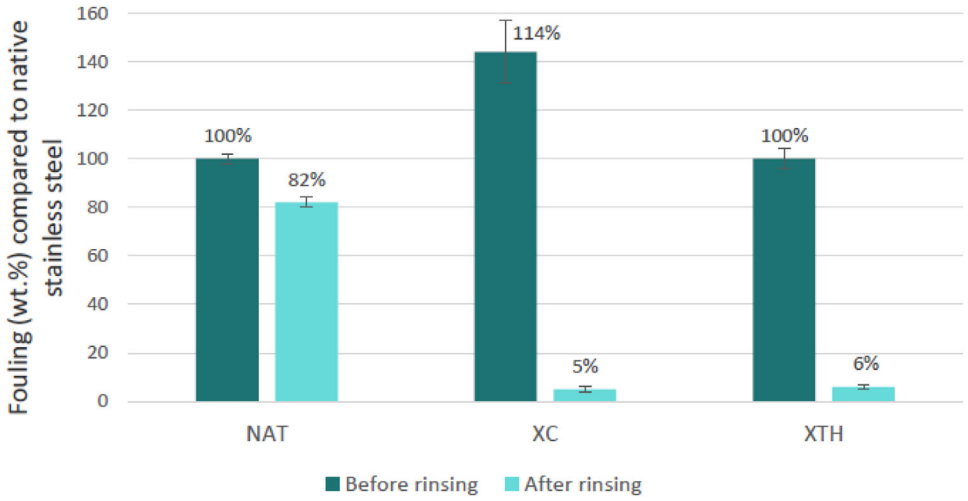

FIGURE 18 Fouling performances after fouling test and after rinsing (Zouaghi, 2018)

(2018) have investigated commercial graphite-based composites revealing promising fouling-release performances. Two types of composites were tested to mitigate dairy fouling: XC samples corresponding to a combination of artificial graphite with pitch binder submitted to carbonisation and XTH samples corresponding to a combination of artificial graphite with PTFE binder. Both XC and XTH samples presented higher SFE than NAT; however, both types exhibited much lower polar component, that is 0.6 and 0 mN/m for XC and XTH, respectively. These surfaces underwent 1.5 hr of pasteurization followed by 20 min of water rising at 85°C. Fouling amounts were assessed before and after water rinsing and the obtained results are depicted in Figure 18. On one hand, before water rinsing, both XC and XTH surfaces presented a fouling increase compared to NAT. On the other hand, the water rinsing led to a fouling drop for both types of composite (less than 10 mg/cmš against 75 mg/cmš for NAT). These results are very encouraging and, furthermore, their high thermal conductivity and lightness make graphite-based materials interesting candidates for replacing SS. Nevertheless, this investigation did not indicate the durability of fouling-release properties of the graphite-based composite after several pasteurization runs.

Silicon-based coatings, developed by Zouaghi et al. (2018), exihibited good fouling-release properties with water rinsing only. These coatings were deposited onto SS using an APP torch as described in Section 3.2.2. Several coatings were obtained by varying the manufacturing parameters. After 1.5 hr of pasteurization, the coated surfaces were submitted to water rinsing at 85°C for 20 min and demonstrated oustanding results with a fouling reduction ranging from 90% to 99%. Nonetheless, after a second fouling run followed by water rinsing, some of the modified surfaces were more fouled than SS surface and other displayed loss of their fouling-release character. On the other hand, a coating, corresponding to certain manufacturing parameters, presented good fouling-release properties, decreasing fouling up to 92%. However, Zouaghi et al. (2018) have demonstrated that the fouling-release properties of silicon-based surfaces are not due to the SFE, which is close to that of SS, or to the polar component, which is higher than that of SS, but can be explained by the formation of uneven nanoparticles providing nanorough surfaces as showed in Figure 19. Despite their low durability, which could be increased by optimising plasma manufacturing parameters, these silicon-based coatings present interesting fouling-release properties, whereras their deposition process is quick compared to PECVD processes. The deposition of a coating on a SS PHE (530 mm × 180 mm) could take around 60 s at maximal scanning speed (300 mm/s).

4.4 | Anti-fouling and fouling-release surfaces

4.4.1 | Amphiphilic surfaces

Amphiphilic surfaces were developed to obtain new materials being both anti-fouling and fouling-release. Hence, this type of surface includes hydrophobic and hydrophilic areas. By designing micro- or nano-hydrophilic and hydrophobic regions, the surface becomes ambiguous, making biomolecules adhesion unfavourable (Gudipati et al., 2005; Kumar et al., 2011). These amphiphilic surfaces have been mainly investigated against biofouling and proven efficient. Galli and Martinelli (2017) reviewed different pathways to realise amphiphilic coatings. Furthermore, some studies reported by Mérian and Goddard

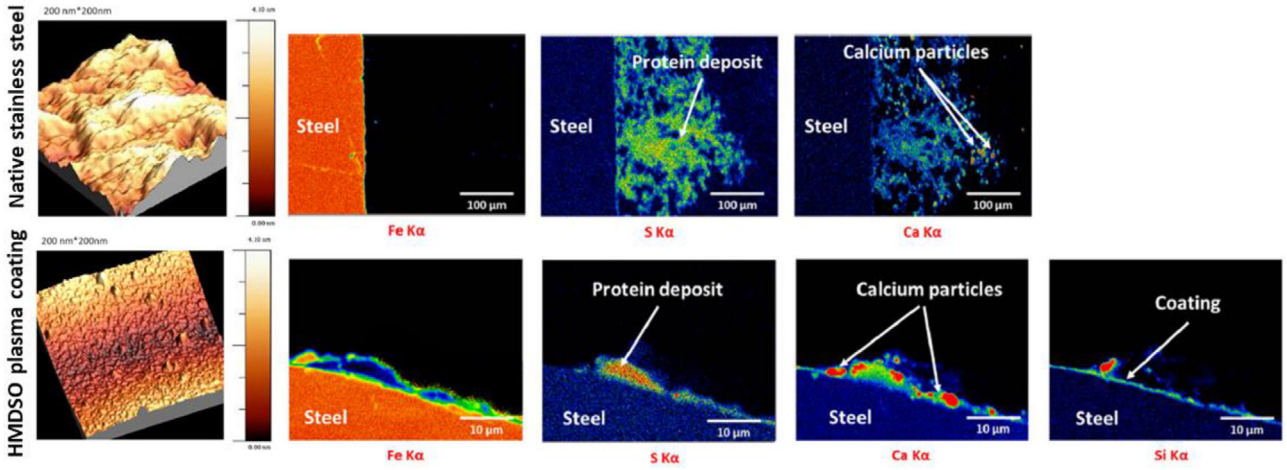

FIGURE 19 AFM pictures of native stainless-steel surface and HMDSO plasma coating (left) and cross-section EPMA X-ray (Electron Probe Microanalysis) mappings demonstrating good fouling-release performances of HMDSO plasma coating (right) (Zouaghi et al., 2018)
Note: Reprinted with permission from Elsevier B.V.

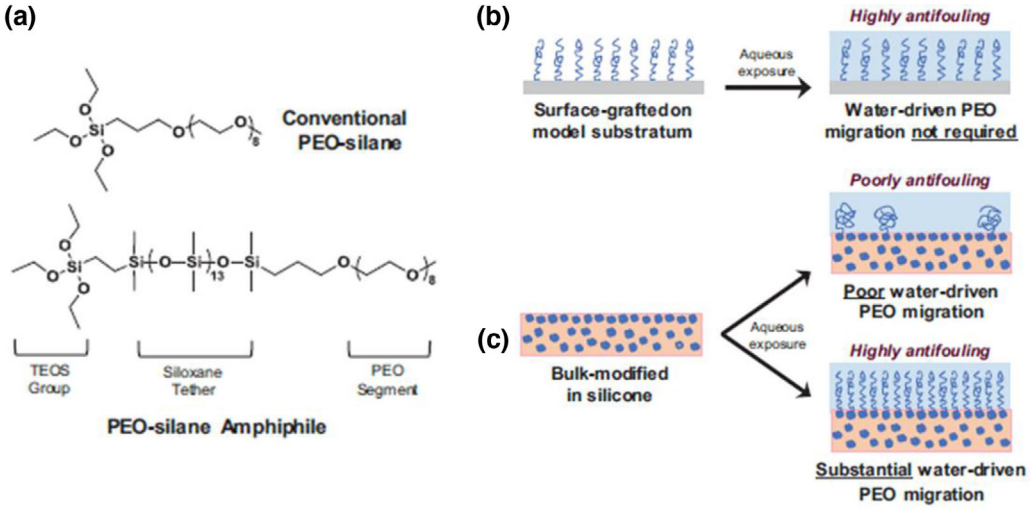

FIGURE 20 (a) Conventional PEO–silane and PEO–silane amphiphile developed by Hawkins et al. (b) Behavior of conventional PEO–silane when it is exposed to aqueous medium. (c) Behavior of conventional PEO–silane in silicone matrix versus PEO–silane amphiphile in silicone matrix when it is exposed to aqueous medium (Zouaghi et al., 2018)
Note: Reprinted with permission from Taylor & Francis.

(2012) have demonstrated the ability of amphiphilic coatings to prevent the adsorption of a range of proteins. According to Mérian and Goddard (2012), the amphiphilic aspect is given either by hydrophobic and hydrophilic monomer parts in the copolymer or by amphiphilic end chains on the polymer backbone. Nonetheless, in most of these amphiphilic coatings, the hydrophobic part is composed of fluorinated groups such as perfluoroalkyl chains. These ones can degrade and form perfluroalkyl acids which have toxicological effects. Few examples of fluorine-free hydrophobic part in amphiphilic coatings have been published, replacing fluorine groups either by alkyl groups or polysiloxane networks such as polydimethylsiloxane (PDMS) (Chen & Thayumanavan, 2009; Cho et al., 2011; Sundaram et al., 2011; Zhou et al., 2014). Anti-fouling and fouling-release properties in amphiphilic coatings were optimized following specific ratios of hydrophilic and hydrophobic moieties. Hawkins et al. (2014), Hawkins et al. (2017), Rufin et al. (2015; 2016) and Faÿ et al. (2016) synthesized an amphiphilic molecule that is a PEG–siloxane with

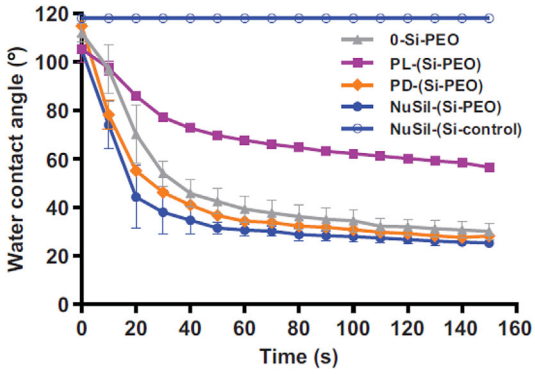

FIGURE 21 Variation of WCA over time of the different pre-treated Si–PEO surfaces: PL and PD corresponding to plasma and polydopamine; NuSil is a commercial primer (Zouaghi et al., 2018)

Note: Reprinted with permission from Taylor & Francis.

cross-linkable triethoxy end groups (Figure 20a), which was incorporated in an elastomeric matrix enhancing PEG resistance and stability (Figure 20c). Studies of PEG and siloxane chain length were carried out. Increasing siloxane tether length reduces the formation of biofilms by improving the mobility of PEG chains. This is not the case for PEG chain length: shorter PEG units do not confer hydrophilic properties and longer PEG units present limited mobility in the matrix.

To date, only one group used an amphiphilic coating to reduce dairy deposits. Based on the development of amphiphilic coatings of Grunlan's team, Zouaghi et al. (2018) used amphiphilic coating onto SS samples and PHE to perform isothermal and in situ fouling tests, respectively. They also assessed the adhesion of the amphiphilic coating using various techniques such as plasma activation, polydopamine coating and commercial primer (NuSil SP 120). The variation of WCA over time was assessed: as displayed in Figure 21, at t_0, the WCA for all surfaces stand between 105 and 115°, demonstrating hydrophobic character. After 150 s, non-pre-treated surfaces and polydopamine and primer pre-treated surfaces exhibited a lower WCA value, around 30°, indicating the migration of polyethylene oxide (PEO) segments at the interface.

These surfaces were tested against a whey protein and calcium solution under continuous flow conditions for 1.5 hr in the pilot PHE. After a single pasteurization cycle, non-pre-treated surfaces were removed from sample holders without dairy deposits, contrary to NAT surfaces, as shown in Figure 22. Promising results were obtained for primed Si–PEO surfaces. This type of surface remained unfouled even after five pasteurization cycles. Therefore, a SS heat exchanger plate (plate number 8) was pre-treated with the commercial primer, coated with the Si–PEO amphiphile and tested in situ for 1.5 hr. No trace of dairy deposit was observed on the eighth plate, thus indicating that this amphiphilic coating has great anti-fouling properties and that PEO chains migrate at the interfaces even when the surface undergoes temperature changes (Figure 22).

Zouaghi et al. (2018) have proven the efficiency of amphiphilic Si–PEO coating in the mitigation of dairy deposits. This type of coating seems to be promising for food industries and presents numerous advantages: PEO is food compatible, and excellent anti-fouling properties are preserved after 7.5 hr of pasteurization and under temperature changes. Nonetheless, after five pasteurization cycles, the thickness of the Si–PEO surfaces decreased, showing erosion during the process. Moreover, the primer used, NuSil SP 120, is classified as carcinogenic mutagenic reprotoxic, which could cause health issues. The effectiveness of the amphiphilic coating after CIP procedures was assessed after 7.5 hr of pasteurization (five fouling runs). It can be observed in Figure 22 that anti-fouling performance was negatively affected. Thus, further researches have to be carried out to improve resistance to shear stress.

4.4.2 | Slippery liquid-infused porous surfaces

Few years ago, SLIPSs were developed by Aizenberg's group (Epstein et al., 2012; Wong et al., 2011). These surfaces are bio-inspired by *Nepenthes* pitcher plants which have a slippery area allowing catching and trapping their food. Observations of insects placed on *Nepenthes* plants showed that the inner waxy pitcher wall is the most important zone to capture insects. This waxy area has anisotropic structures trapping insects from adhesive secretion (Bohn & Federle, 2004). This feature has attracted attention to design anti-fouling coatings. SLIPSs consist porous or nanostructured surfaces impregnated by low-surface-energy lubricants. The obtained surface is extremely smooth, homogeneous and slippery (Figure 23). Usually, SLIPSs have low CAH (<2°) and low sliding angle. Thus, fluids and biological fouling cannot hold on the surface and slide off.

Nonetheless, designing such materials can be complex and several ways are reported in the literature to design such surfaces. The elaboration of SLIPS is based on three principles in order to obtain a smooth and stable liquid surface: (i) the lubricant must have a higher chemical affinity for the underlying support than for the surrounding medium, (ii) nano- or micro-structured substrate improves the lubricant immobilization and retention through Van der Waals and capillarity forces and (iii) the lubricant should be immiscible with the surrounding

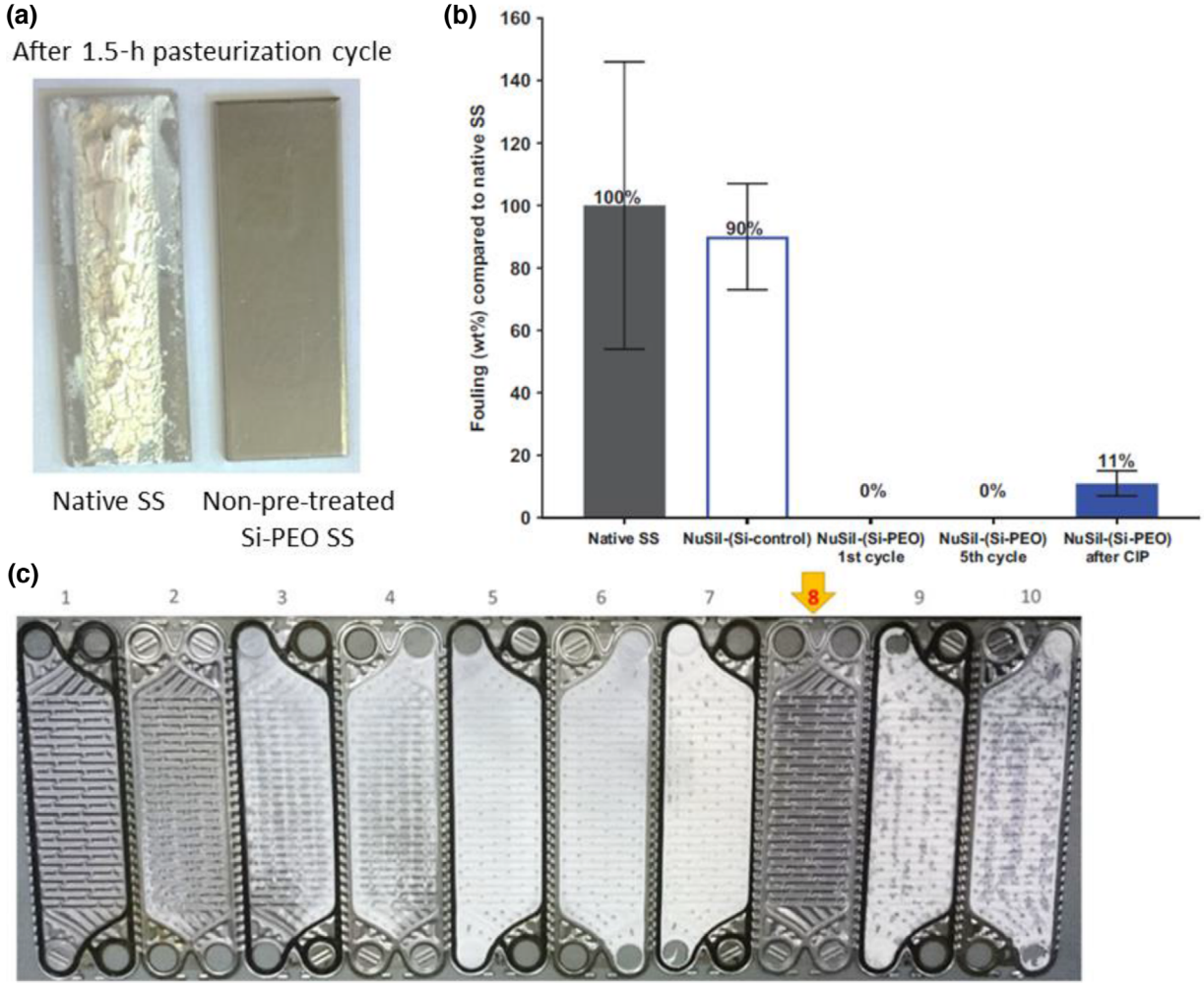

FIGURE 22 (a) Fouling deposit onto native stainless steel and amphiphilic coating under isothermal conditions, (b) anti-fouling of amphiphilic coating and (c) fouling deposit onto V7 plate heat exchanger under in situ conditions (Zouaghi et al., 2018)
Note: Reprinted with permission from Taylor & Francis.

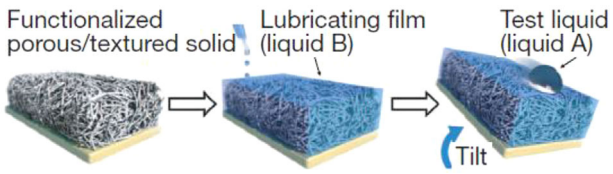

FIGURE 23 Fabrication of slippery liquid-infused porous surface (Wong et al., 2011)
Note: Reprinted with permission from Springer.

medium (Howell, Grinthal, Sunny, Aizenberg & Aizenberg, 2018).

In the literature, most papers deal with the design of SLIPS for anti-fouling applications against microorganisms and microalgae in the marine sector or against blood and bacteria in the medical sector. For instance, Epstein et al. (2012) have proven that such slippery surfaces were more efficient than PEGylated surfaces by preventing biofilm adhesion up to 99% under low flow conditions.

As for the amphiphilic coating, only one work has been done on the development of SLIPS against dairy fouling deposits. Recently, Zouaghi et al. (2017) have fabricated SLIPS-like surfaces with good anti-fouling and encouraging fouling-release properties. SLIPS-like surfaces were elaborated in several steps that have been detailed in Section 3.2.3. As in most studies, a perfluorinated oil was chosen as lubricant (DuPont Krytox GPL 103). CAH measurements confirmed the slippery feature of these SLIPS-like surfaces, giving a CAH of 0.6° and a sliding angle of 2°. After 1.5 hr of pasteurization test at 85°C, SLIPS-like surfaces exhibited a fouling decrease up to 63% and, as depicted in Figure 24, dairy deposit seems to be less adherent onto slippery surfaces than onto NAT. Thus, these surfaces underwent another fouling run followed by a water rinsing, corresponding to 'SLIPS-r' in Figure 24. The rinsed

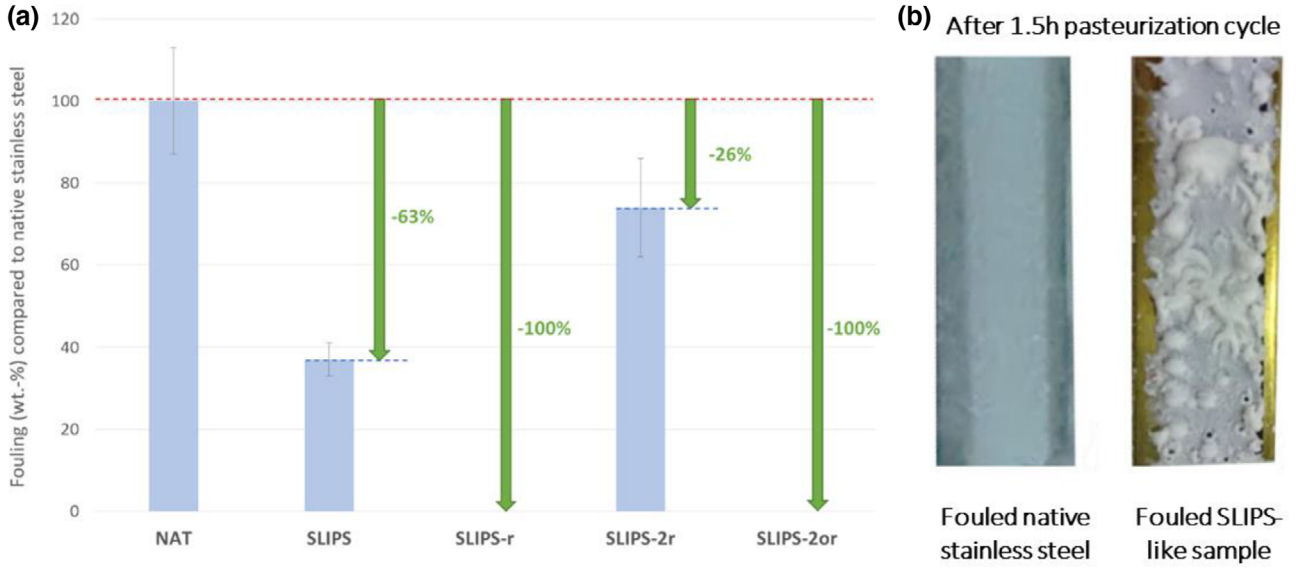

FIGURE 24 (a) Anti-fouling and fouling-release performances of SLIPS-like surface. (b) Physical aspect of dairy fouling onto SLIPS-like sample compared to that onto native stainless steel after 1.5-hr pasteurization (Zouaghi et al., 2017)
Note: Reprinted with permission from American Chemical Society.

slippery surfaces were totally clean, demonstrating exceptional fouling-release properties.

These results are very promising and manifest a real potential to reduce dairy fooling due to both anti-fouling and fouling-release properties. Furthermore, SLIPS-like surfaces present environmental and economic advantages owing to a 'greener' cleaning step, that is, requiring water only. However, as observed by other groups, Zouaghi et al. (2017) noticed a lubricant loss during the run, leading to a loss of fouling-release performance. In order to improve lubricant retention, some authors recently proposed a solution using the PDMS layer, either as a vascularized substrate by creating channels in PDMS matrix or grafted to the substrate. PDMS has also been used in brush or as a matrix to graft the lubricant. But these solutions were not assessed under high flow conditions (Howell et al., 2014; Jing & Guo, 2019; Zhang et al., 2018; Zhang et al., 2018). Another drawback is the non-food grade of the fluorinated lubricant which should be replaced by pharmaceutical-grade oils, silicone oil or vegetable oils. Several works have been published on this latter type of oils, but not applied in the dairy fouling field (Manabe et al., 2015; Manna & Lynn, 2015; Nishioka et al., 2016; Togasawa et al., 2018).

5 | DISCUSSION

Dairy fouling depends on several factors such as product characteristics, process parameters and surface properties. For this reason, in this review, studies in batch conditions have been separated from those in continuous flow to investigate the impact of surface properties. However, it appears that the comparison of the impact of surface properties remains intricate due to numerous process parameters, model fluids and cleaning conditions used in fouling tests whatever the process equipment used to evaluate the surface. Based on the knowledge of industrial habits and former studies, a standardization of model fluid for fouling tests, process parameters, surface characterizations and cleaning conditions could make comparisons more meaningful. For instance, different techniques are proposed to systematically characterise coatings and/or materials. A classification of cleaning conditions is also proposed to evaluate the fouling-release behavior of the tested coatings and/or materials in order to mitigate fouling deposition.

5.1 | Model fluid and process parameters

As shown in Tables 3 and 4, various types of fluid have been used: β-Lg in phosphate buffer solution, WPC with or without calcium ($CaCl_2$), WPI with or without calcium (SMUF) and whole, raw, skim or pasteurized milk. For these fluids, not only the composition in proteins (whey only or mixture of casein/whey) and in mineral (mainly the type of calcium complex – Ca^{2+}, $CaHPO_4$, $Ca_3(PO_3)_2$, $CaCO_3$… – depending both on the presence of chelating agents such as phosphate ions and citrate and physico–chemical conditions such as pH and temperature in the dairy derivative)

but also the content in carbohydrate (lactose) and lipids is very different.

Consequently, depending on the fluid composition, the concentration balance of species (protein and/or mineral) in the bulk can be seriously affected and may significantly alter the fouling layer build-up (Blanpain-Avet et al., 2020; Liu et al., 2020; Scudeller et al., 2021).

Ignoring the effect of carbohydrate and lipids on fouling which has been less investigated, currently, it is widely admitted that protein denaturation and salts precipitation of calcium element are the two major underlying mechanisms responsible for fouling, but the exact pathways by which proteins and calcium salts interact and feed the layer of deposit onto SS surface are far from being wholly understood.

For WPI solutions, when phosphate ions content is low, it seems that free ionic calcium content actively participates in the formation of the fouling layer but calcium carbonate (Jimenez et al., 2013) and calcium phosphate (Blanpain-Avet et al., 2020; Dupeyrat et al., 1987; Khaldi et al., 2018; Scudeller et al., 2021) have also been mentioned when phosphate ions content increases.

For dairy derivatives which are mixtures of whey protein (WP) and casein (as the case of milk containing 80% casein and 20% WP), fouling mechanisms are less demystified. As explained by Liu et al., the presence of casein micelles in milk makes more complex the possibilities of protein aggregation and salts precipitation as they constitute both a source of proteins (alpha, beta, kappa caseins) and of mineral elements through their calcium phosphate nanoclusters which can also modify the calcium balance between colloidal and soluble phases (Liu et al., 2020). The understanding of mineral/protein interaction is better in whey, which could be considered as a simpler protein solution than milk due to the absence of casein micelles.

Consequently, depending on the fluid composition, interactions with surfaces could also differ for a given temperature as shown by Rosmaninho et al. (2008) and later by Blanpain-Avet et al. (2020) and Scudeller et al. (2021).

This tricky situation regarding the scientific understanding of fouling mechanism at the molecular level and the fact that continuous flow equipment is not so usual for academic laboratories explain why fouling and cleaning abilities of surface are often tested on a first approach. Then, if coating exhibits good anti-fouling or fouling-release performances, it could be tested against whole or skim milk.

To date, two studies have investigated the fouling deposit onto modified SS or coatings using both whey protein solutions and milk. Patel et al. (2013) performed tests in batch conditions using skim milk and WPI solution to foul 2B 316L SS and DLC surfaces at pasteurization temperature. A lower fouling mass was observed with WPI solution DLC surfaces. Therefore, at pasteurization temperature, whey protein solution and milk can lead to fouling deposit with close composition; however, it seems that interactions between surfaces and fluids (milk or whey protein solutions) differ. This has been corroborated by Magens' (2019) work. Raw milk and whey protein solution were used in continuous flow at pasteurization temperature, fouling 2R 304 SS surface and FEP coating. With WP solution, the calcium fraction is the same in fouling deposit onto SS surface (5.1 mg/g) and FEP coating (6.6 mg/g), but differs using milk. A higher calcium fraction is found into fouling onto SS surface, 92.3 mg/g, against 74.1 mg/g onto FEP coating. Thus, this demonstrates that more investigations should be carried out on both model fluids and milk to confirm the effectiveness of new coatings at mitigating fouling deposit.

Fouling behavior was assessed through a large variety of apparatuses such as heating rod, rotating disk apparatus, flow cell, benchtop PHE or PHE. Hence, different process parameters such as (i) bulk and surface temperatures in batch, (ii) inlet and outlet temperatures in continuous flow and (iii) hydrodynamic conditions have been used even in similar configurations.

Hydrodynamic conditions are characterized by flow regime or flow rate and the hydrodynamic regime is seldom reported. In dairy industries, the flow is turbulent to ensure a homogeneous thermal treatment, moreover, in turbulent regime, wall shear stresses increase, inducing fouling removal (Belmar-Beiny et al., 1993). Some authors have also proven that Reynolds number influences aggregate size and fouling deposit structure. de Guibert et al. (2020) found larger aggregate in transient regimes than in laminar or turbulent regimes, corroborating works of Simmons et al. (2007) and Wolz et al. (2016). Moreover, Guérin et al. (2007) observed that the structure of fouling deposit appears denser from Re = 3200 in connection with smaller aggregates size. Nevertheless, it has been also demonstrated that heating temperature has a stronger impact on protein aggregation. Finally, although aggregate size depends on flow regime, this dependency decreases with raising temperature (de Guibert et al., 2020; Petit et al., 2013; Simmons et al., 2007). Because a large variety of apparatuses is used and as the equipment geometry affects flow regime, standardization of process parameters remains complex. Therefore, these parameters, and especially the flow regime, should be systematically notified.

5.2 | Surface characterizations

By modifying SS surface with a coating or using other types of materials, studies have demonstrated fouling reduction and/or fouling removal improvement. The investigations of the influence of SFE and R_a on dairy fouling behavior in both batch and continuous flow conditions led to

similar conclusions. Three trends can be identified from the analysis of the literature: (i) initially, some authors agreed that SFE only impacts fouling deposit, (ii) based on Baier's relationship (Baier, 2006), an optimal SFE value may tend to mitigate whey protein adhesion, otherwise, Boxler et al. (2013) suggested the existence of an optimal electron donor value and (iii) finally, another group of authors stated that both SFE and R_a act on dairy fouling. However, for these three trends, no clear correlations have been established.

The lack of information regarding SFE, R_a or wettability makes the comparison difficult between coatings tested against dairy fouling behavior. Globally, coatings and materials have been characterized by SFE and R_a but, in some works, one of these surface characterizations is missing. In addition, although SFE and R_a are related by wettability, few works have evaluated this latter parameter and none of them reported the potential impact of wettability on fouling or cleaning behaviors. In order to obtain as much information as possible about surface properties, systematic surface analyses should be carried out by providing at least SFE, R_a and wettability.

To go further, different models exists for SFE calculation, and there is no consensus on which one should be used when studying a certain matter, which makes the comparison between results complicated. Among those presented in Section 2.2, the OWRK model is the most used. But results can be slightly different between two models. Boxler (2014) worked on SFE evaluation via two models, OWRK and van Oss, and pointed out very different results: lower polar part (γ^{AB}), higher dispersive component (γ^{LW}) as well as higher total energy (γ^{TOT}) in van Oss approach than in OWRK (γ^{P}, γ^{D}, and γ^{TOT}) (Boxler, 2014). Moreover, according to Hejda et al. (2010), the selection of liquids used for contact angle measurements is more important in van Oss model than in OWRK. In order to corroborate or contradict Boxler's conclusions, SFE should be assessed by both van Oss and OWRK models.

Topography data are mostly measured by profilometer or AFM, and are usually given through one value, which is the arithmetic mean R_a. In food industries, surfaces should present $R_a < 0.8$ μm (Verran & Redfern, 2016). Nevertheless, works exhibit the effectiveness of smoother coatings for mitigating dairy fouling and cleaning, ranging from 0.02 to 0.5 μm (Gordon et al., 1968; Jimenez et al., 2012; Piepiórka Stepuk et al., 2016; Zouaghi et al., 2018). But AFM probes relatively small areas. Besides AFM, R_a should be assessed by dynamic contact angle measurements given by CAH, which depends on R_a and surface heterogeneity. Barish and Goddard (2013) confirmed AFM analyses with CAH measurements, exhibiting that low R_a leads to a low CAH due to a more homogeneous surface. This has been corroborated by Zouaghi et al. (2017). It seems that the lower the CAH, the higher the fouling reduction; however, no correlation has been established yet. Hence, it could be interesting to systematically assess the dynamic contact angle as well.

To date, only one study has considered another surface property: surface charges. Nevertheless, the results on surface charges impact on fouling behavior remain unclear. Indeed, when electrostatic interactions are not neglected (Magens, 2019), the impact of measured surface charges of SS and DLC coatings on fouling behavior is not established (Boxler, 2014).

The adhesion of coatings onto SS is a great issue, which is barely reported. Zouaghi et al. (2018) have assessed the adhesion of amphiphilic coating onto 316L SS surfaces using several techniques: (i) plasma activation, (ii) polydopamine coating, and (iii) commercial primer (NuSil SP 120). The durability of the coating as a function of the adhesion technique was consistent with adhesion cross hatch test. Coating adhesion to SS surfaces should be characterized in order to assess the potential durability of the coating.

5.3 | Cleaning conditions

As previously defined, fouling-release surfaces facilitate fouling removal through shear stress from cleaning. Consequently, fouling-release properties of materials or coatings are assessed through the cleaning step. Nevertheless, as mentioned in Section 4.3, numerous cleaning conditions have been used, thus making the comparison between surfaces complex. Indeed, some studies have only used a mechanical cleaning with water and others have combined both mechanical and chemical cleaning. Zouaghi et al. (2017, 2018, 2018) demonstrated that water rinsing was sufficient in certain cases to drastically remove fouling deposit. Barish and Goddard (2013) also observed a fouling reduction after water rinsing and pointed out a greater mass of fouling removed with a flow rate increase. On the other hand, they emphasized better fouling-release performance using alkaline cleaning. Moreover, and as for fouling tests, it is important to note that in most of studies, cleaning or rinsing conditions are not always detailed. For instance, in Barish's work, temperature of water and duration of cleaning are not specified, although these are two important factors. Investigations have demonstrated that the cleaning rate increases with temperature (Fryer & Christian, 2005; Hankinson & Carver, 1968; Timperley & Smeulders, 1988). Timperley and Smeulders (1988) showed a decrease in cleaning time up to 60% when the cleaning solution temperature rose from 60 to 90°C and up to 40% when the temperature cleaning was comprised between 60 and 75°C.

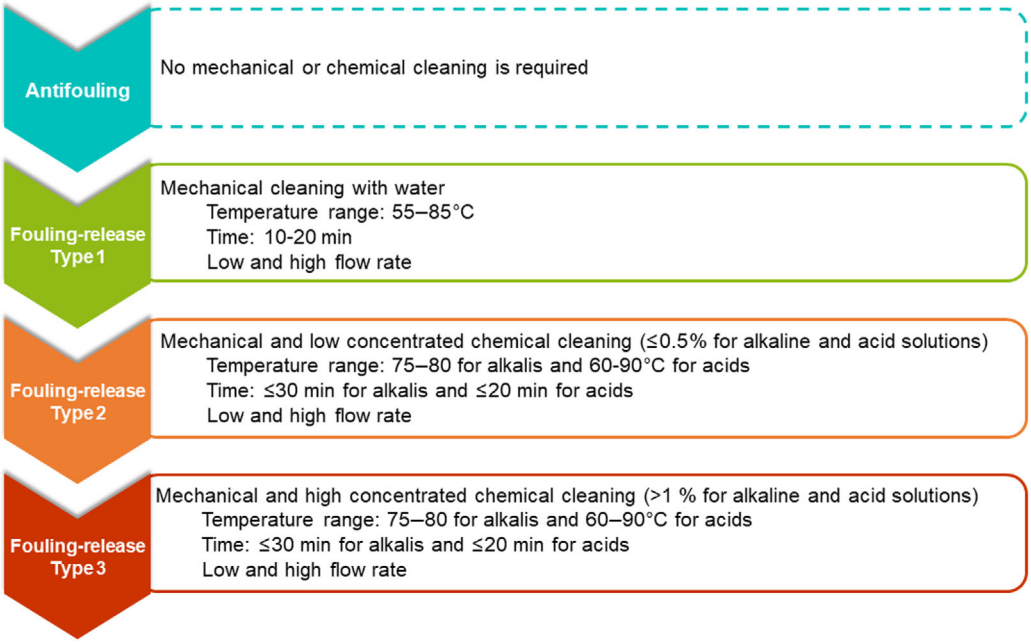

FIGURE 25 Cleaning conditions assessing fouling-release performances

Standardization of cleaning step with specific conditions could allow classifying surfaces as a function of their cleanability, revealing their fouling-release performance. In the same way that anti-fouling performances are probed, the cleanability could be evaluated by weighing the fouling deposit remaining onto surfaces. Other methods (heat transfer measurements, pressure drop, conductivity, pH) allowing to follow the cleaning step have been reviewed by (Goode et al., 2013)

Surfaces could be divided into four groups as displayed in Figure 25. The first group corresponds to anti-fouling surfaces, thus no or less frequent cleaning should be needed. The second category is called fouling-release Type 1, and only mechanical cleaning using water as cleaning solution is required. Temperature and time ranges are based on works of Hankinson and Carver (1968) and Zouaghi et al. (2017, 2018, 2018). Fouling-release Type 2 corresponds to mechanical and chemical cleaning with alkaline and acid solutions less concentrated than in CIP procedures. On the contrary, fouling-release Type 3 corresponds to harder cleaning conditions. For both Type 2 and Type 3, temperature and time are based on CIP procedures detailed by Bylund (1995).

Among these different types of cleaning, it is more difficult to select the flow rate range as various types of fouling test exist. Consequently, a low flow rate corresponds to the same flow rate used for fouling test. High flow rate is two times higher than low flow rate, a distinction based on Barish and Goddard (2013), Rosmaninho et al. (2008) and Beuf et al. (2003) works. This proposed classification is build-up from works having investigated the cleanability of coatings and materials and CIP procedures. Hence, conditions can be modified with further tests. It could be also interesting to assess surface properties after a significant number of fouling and cleaning cycles to evaluate coating aging; it is known that alkaline solution can degrade silica-based coatings.

6 | CONCLUSIONS

The aim of this review was to investigate the impact of surface modifications on fouling and cleaning behaviors.

Generally, the comparison of the impact of surface modification on fouling behavior remains complex due to several points. To begin with, fouling tests are led either in batch or in continuous flow conditions. For both conditions, different model fluids and process parameters are used but not always reported, leading to an intricate interpretation of the real effect of the studied coating. Moreover, surface analyses such as SFE, roughness or wettability are not systematically carried out, leading to the non-complete understanding of the coating effects.

It seems in both batch and continuous flow, a similar conclusion stands out: either SFE or the combination of SFE and roughness reduces final fouling amount or facilitates fouling removal. However, no clear correlation has been yet established. Other molecular interactions as the repulsive electric double layer could be taken into account.

Some fouling-release coatings seem promising as they can be cleaned using water rinsing only. These latter could offer real advantages regarding the environmental and

economic cleaning costs in dairy thermal processing. Nevertheless, the cleanability is assessed through diverse conditions, preventing a good comparability between studies.

Consequently, this review has proposed to standardise the study of modified surfaces mitigating dairy fouling. However, these suggestions are not fixed and can be modified with further investigations.

ACKNOWLEDGMENT

The authors thank the French National Agency (ANR) for its financial supports (ECONOMICS Project ANR-17-CE08-0032).

AUTHOR CONTRIBUTIONS

Manon Saget—Formal analysis; investigation; writing original draft; writing review editing. Caroline Françolle de Almeida—Investigation; methodology. Guillaume Delaplace—Validation; writing review editing. Vincent Thomy—Validation; writing review editing. Yannick Coffinier—Validation; writing review editing. Maude Jimenez—Funding acquisition; supervision; validation; writing review editing.

CONFLICTS OF INTEREST

The authors declare no conflicts of interest.

ORCID

Maude Jimenez https://orcid.org/0000-0002-0372-1503

REFERENCES

Ahn, H. S., Kim, K. M., Lim, S. T., Lee, C. H., Han, S. W., Choi, H., Koo, S., Kim, N., Jerng, D., & Wongwises, S. (2019). Anti-fouling performance of chevron plate heat exchanger by the surface modification. *International Journal of Heat and Mass Transfer*, *144*, 118634. https://doi.org/10.1016/j.ijheatmasstransfer.2019.118634

Al-Janabi, A., Malayeri, M. R., & Müller-Steinhagen, H. (2010). Experimental fouling investigation with electroless Ni-P coatings. *International Journal of Thermal Sciences*, *49*(6), 1063–1071. https://doi.org/10.1016/j.ijthermalsci.2009.05.009

Albert, F., Augustin, W., & Scholl, S. (2011). Roughness and constriction effects on heat transfer in crystallization fouling. *Chemical Engineering Science*, *66*(3), 499–509. https://doi.org/10.1016/j.ces.2010.11.021

Laschewsky A. (2014). Structures and synthesis of zwitterionic polymers. *Polymers*, *6*, 1544–1601.

Asuri, P., Karajanagi, S. S., Kane, R. S., & Dordick, J. S. (2007). Polymer-nanotube-enzyme composites as active antifouling films. *Small*, *3*(1), 50–53. https://doi.org/10.1002/smll.200600312

Augustin, W., Geddert, T., & Scholl, S. (2007). Surface treatment for the mitigation of whey protein fouling. In H. Müller-Steinhagen, M. Reza Malayeri, & A. P. Watkinson (Eds.), *Heat exchanger fouling and cleaning VII* (pp. 206–214). Engineering Conferences International.

Baier, R. E. (2006). Surface behaviour of biomaterials: The theta surface for biocompatibility. *Journal of Materials Science: Materials in Medicine*, *17*(11), 1057–1062. https://doi.org/10.1007/s10856-006-0444-8

Balasubramanian, S., & Puri, V. M. (2008). Fouling mitigation during product processing using a modified plate heat exchanger surface. *American Society of Agricultural and Biological Engineers*, *51*(2), 629–639.

Balasubramanian, S., & Puri, V. M. (2009). Reduction of milk fouling in a plate heat exchanger. *American Society of Agricultural and Biological Engineers*, *52*(5), 1603–1610.

Banerjee, I., Pangule, R. C., & Kane, R. S. (2011). Antifouling coatings: Recent developments in the design of surfaces that prevent fouling by proteins, bacteria, and marine organisms. *Advanced Materials*, *23*(6), 690–718. https://doi.org/10.1002/adma.201001215

Bansal, B., & Chen, X. D. (2006). A critical review of milk fouling in heat exchangers. *Comprehensive Review in Food Science and Food Safety*, *5*, 27–33. https://doi.org/10.1111/j.1541-4337.2006.tb00080.x

Barish, J. A., & Goddard, J. M. (2013). Anti-fouling surface modified stainless steel for food processing. *Food and Bioproducts Processing*, *91*(4), 352–361. https://doi.org/10.1016/j.fbp.2013.01.003

Belmar-Beiny, M. T., & Fryer, P. J. (1993). Preliminary stages of fouling from whey protein solutions. *Journal of Dairy Research*, *60*(4), 467–483. https://doi.org/10.1017/S0022029900027837

Belmar-Beiny, M. T., Gotham, S. M., Paterson, W. R., Fryer, P. J., & Pritchard, A. M. (1993). The effect of Reynolds number and fluid temperature in whey protein fouling. *Journal of Food Engineering*, *19*(2), 119–139. https://doi.org/10.1016/0260-8774(93)90038-L

Beuf, M., Rizzo, G., Leuliet, J. C., Müller-Steinhagen, H., Yiantsios, S., Karabelas, A., & Benezech, T. (2003). Fouling and cleaning of modified stainless steel plate heat exchangers processing milk products. In A. P. Watkinson, H. Müller-Steinhagen, & M. R. Malayen (Eds.), *Heat exchanger fouling and cleaning fundamentals and applications* (pp. 1–8). Engineering Conferences International.

Blanpain-Avet, P., André, C., Azevedo-Scudeller, L., Croguennec, T., Jimenez, M., Bellayer, S., Six, T., Martins, G. A. S., & Delaplace, G. (2020). Effect of the phosphate/calcium molar ratio on fouling deposits generated by the processing of a whey protein isolate in a plate heat exchanger. *Food and Bioproducts Processing*, *121*, 154–165. https://doi.org/10.1016/j.fbp.2020.02.005

Bohn, H. F., & Federle, W. (2004). Insect aquaplaning: Nepenthes pitcher plants capture prey with the peristome, a fully wettable water-lubricated anisotropic surface. *Proceedings of the National Academy of Sciences*, *101*(39), 14138–14143. https://doi.org/10.1073/pnas.0405885101

Bohnet, M. (1987). Fouling of heat transfer surfaces. *Chemical Engineering & Technology*, *10*, 113–125.

Bormashenko, E. (2009). Young, Boruvka-Neumann, Wenzel and Cassie-Baxter equations as the transversality conditions for the variational problem of wetting. *Colloids and Surfaces A: Physicochemical and Engineering Aspects*, *345*(1–3), 163–165. https://doi.org/10.1016/j.colsurfa.2009.04.054

Bott, T. R. (2011). *Industrial biofouling*. Elsevier.

Boxler, C. (2014). *Fouling by milk constituents and cleaning of modified surfaces*. Technischen Universität Carolo-Whilhelmina zu Braunschweig.

Boxler, C., Augustin, W., & Scholl, S. (2013a). Fouling of milk components on DLC coated surfaces at pasteurization and UHT temperatures. *Food and Bioproducts Processing*, *91*(4), 336–347. https://doi.org/10.1016/j.fbp.2012.11.012

Boxler, C., Augustin, W., & Scholl, S. (2013b). Influence of surface modification on the composition of a calcium phosphate-rich whey protein deposit in a plate heat exchanger. *Dairy Science and Technology*, *94*(1), 17–31. https://doi.org/10.1007/s13594-013-0142-5

Boxler, C., Kaup, F., Teixeira, R., Pereira, A., Mendes, J., Melo, L. F., Augustin, W., & Scholl, S. (2011). On-line monitoring of deposition and removal of milk salts on coated surfaces. In M. R. Malayeri, H. Müller-Steinhagen & A. P. Watkinson (Eds.), *Heat exchanger fouling and cleaning* (pp. 429–432). Engineering Conferences International.

Britten, M., Green, M. L., Boulet, M., & Paquin, P. (1988). Deposit formation on heated surfaces: Effect of interface energetics. *Journal of Dairy Research*, *55*(4), 551–562. https://doi.org/10.1017/S0022029900033331

Burton, H. (1967). Seasonal variation in deposit formation from whole milk on a heated surface. *Journal of Dairy Research*, *34*(2), 137–143. https://doi.org/10.1017/S0022029900012267

Burton, H. (1968). Section G. Deposits from whole milk in heat treatment plant—A review and discussion. *Journal of Dairy Research*, *35*(2), 317–330. https://doi.org/10.1017/S0022029900019038

Bylund, G. (1995). Cleaning of dairy equipment. In A. B. Teknotext (Ed.), *Dairy processing handbook* (pp. 403–414). Tetra Pak Processing Systems AB.

Carter, B. G., Cheng, N., Kapoor, R., Meletharayil, G. H., & Drake, M. A. (2021). Invited review: Microfiltration-derived casein and whey proteins from milk. *Journal of Dairy Science*, *104*(3), 2465–2479. https://doi.org/10.3168/jds.2020-18811

Cassie, A. B. D., & Baxter, S. (1944). Of porous surfaces. *Transactions of the Faraday Society*, *40*(5), 546–551. https://doi.org/10.1039/tf9444000546

Changani, S. D., Belmar-Beiny, M. T., & Fryer, P. J. (1997). Engineering and chemical factors associated with fouling and cleaning in milk processing. *Experimental Thermal and Fluid Science*, *14*(4), 392–406. https://doi.org/10.1016/S0894-1777(96)00141-0

Chen, Y., & Thayumanavan, S. (2009). Amphiphilicity in homopolymer surfaces reduces nonspecific protein adsorption. *Langmuir*, *25*(24), 13795–13799. https://doi.org/10.1021/la901692a

Cho, Y., Sundaram, H. S., Weinman, C. J., Paik, M. Y., Dimitriou, M. D., Finlay, J. A., Callow, M. E., Callow, J. A., Kramer, E. J., & Ober, C. K. (2011). Triblock copolymers with grafted fluorine-free, amphiphilic, non-ionic side chains for antifouling and fouling-release applications. *Macromolecules*, *44*(12), 4783–4792. https://doi.org/10.1021/ma200269s

de Guibert, D., Hennetier, M., Martin, F., Six, T., Gu, Y., Le Floch-Fouéré, C., Delaplace, G., & Jeantet, R. (2020). Flow process and heating conditions modulate the characteristics of whey protein aggregates. *Journal of Food Engineering*, *264*, 109675. https://doi.org/10.1016/j.jfoodeng.2019.07.022

De Jong, P. (1997). Impact and control of fouling in milk processing. *Trends in Food Science and Technology*, *8*(12), 401–405. https://doi.org/10.1016/S0924-2244(97)01089-3

De Wit, J. N. (1990). Thermal stability and functionality of whey proteins. *Journal of Dairy Science*, *73*(12), 3602–3612. https://doi.org/10.3168/jds.S0022-0302(90)79063-7

Delplace, F., Leuliet, J. C., & Levieux, D. (1997). A reaction engineering approach to the analysis of fouling by whey proteins of a six-channels-per-pass plate heat exchanger. *Journal of Food Engineering*, *34*(1), 91–108. https://doi.org/10.1016/S0260-8774(97)00068-X

Delsing, B. M. A., & Hiddink, J. (1983). Fouling of heat transfer surfaces by dairy liquids. *Netherlands Milk & Dairy Journal*, *37*, 139–148.

Derjaguin, B., & Landau, L. (1941). Theory of the stability of strongly charged lyophobic sols and of the adhesion of strongly charged particles in solutions of electrolytes. *Acta Physico Chemica URSS*, *14*, 633–662.

Detry, J. G., Sindic, M., & Deroanne, C. (2010). Hygiene and cleanability: A focus on surfaces. *Critical Reviews in Food Science and Nutrition*, *50*(7), 583–604. https://doi.org/10.1080/10408390802565913

Dey, A., Bomans, P. H. H., Müller, F. A., Will, J., Frederik, P. M., De With, G., & Sommerdijk, N. A. J. M. (2010). The role of prenucleation clusters in surface-induced calcium phosphate crystallization. *Nature Materials*, *9*(12), 1010–1014. https://doi.org/10.1038/nmat2900

Dhillon, M. (2012). *The effect of silver ion-implantation of stainless steel on bacterial adhesion and biofilm formation*. Massey University.

Dimitrakellis, P., & Gogolides, E. (2018). Hydrophobic and superhydrophobic surfaces fabricated using atmospheric pressure cold plasma technology: A review. *Advances in Colloid and Interface Science*, *254*, 1–21. https://doi.org/10.1016/j.cis.2018.03.009

Donnet, C. (1998). Recent progress on the tribology of doped diamond-like and carbon alloy coatings: A review. *Surface and Coatings Technology*, *100–101*(1–3), 180–186. https://doi.org/10.1016/S0257-8972(97)00611-7

Dupeyrat, M., Labbé, J.-P., Michel, F., Billoudet, F., & Daufin, G. (1987). Mouillabilité et interactions solide-liquide dans l'encrassement de divers matériaux par du lactosérum et du lait. *Le Lait*, *67*(4), 465–486. https://doi.org/10.1051/lait:1987428

Epstein, A. K., Wong, T. S., Belisle, R. A., Boggs, E. M., & Aizenberg, J. (2012). Liquid-infused structured surfaces with exceptional anti-biofouling performance. *Proceedings of the National Academy of Sciences of the United States of America*, *109*(33), 13182–13187. https://doi.org/10.1073/pnas.1201973109

Epstein, N. (1983). Thinking about heat transfer fouling: A 5 × 5 matrix. *Heat Transfer Engineering*, *4*(1), 43–56. https://doi.org/10.1080/01457638108939594

Eral, H. B., 'T Mannetje, D. J. C. M., & Oh, J. M. (2013). Contact angle hysteresis: A review of fundamentals and applications. *Colloid and Polymer Science*, *291*(2), 247–260. https://doi.org/10.1007/s00396-012-2796-6

Faÿ, F., Hawkins, M. L., Réhel, K., Grunlan, M. A., & Linossier, I. (2016). Non-toxic, anti-fouling silicones with variable PEO – Silane amphiphile content. *Green Materials*, *4*(2), 53–62.

Fickak, A., Al-Raisi, A., & Chen, X. D. (2011). Effect of whey protein concentration on the fouling and cleaning of a heat transfer surface. *Journal of Food Engineering*, *104*(3), 323–331. https://doi.org/10.1016/j.jfoodeng.2010.11.004

Förster, M., Augustin, W., & Bohnet, M. (1999). Influence of the adhesion force crystal/heat exchanger surface on fouling mitigation. *Chemical Engineering and Processing: Process Intensification*, *38*(4–6), 449–461. https://doi.org/10.1016/S0255-2701(99)00042-2

Foster, C. L., & Green, M. L. (1989). A model heat-exchange apparatus for the investigation of fouling of stainless steel surfaces by milk I. Deposit formation at 100°C. *Journal of Dairy Research*, *56*(2), 201–209. https://doi.org/10.1017/S002202990002642X

Fowkes, F. M. (1964). Attractive forces at interfaces. *Industrial and Engineering Chemistry*, *56*(12), 40–52. https://doi.org/10.1109/CHICC.2008.4605198

Fryer, P. J., & Belmar-Beiny, M. T. (1991). Fouling of heat exchangers in the food industry: A chemical engineering perspective. *Trends in Food Science and Technology*, *2*, 33–37. https://doi.org/10.1016/0924-2244(91)90611-L

Fryer, P. J., & Christian G. K. (2005). Improving the cleaning of heat exchangers. In H. L. M. Lelieveld, M. A. Mostert, & J. Holah (Eds.), *Handbook of hygiene control in the food industry* (pp. 468–496). Woodhead Publishing.

Gadelmawla, E. S., Koura, M. M., Maksoud, T. M. A., Elewa, I. M., & Soliman, H. H. (2002). Roughness parameters. *Journal of Materials Processing Technology*, *123*(1), 133–145. https://doi.org/10.1016/S0924-0136(02)00060-2

Galli, G., & Martinelli, E. (2017). Amphiphilic polymer platforms: Surface engineering of films for marine antibiofouling. *Macromolecular Rapid Communications*, *38*(8), 8–12. https://doi.org/10.1002/marc.201600704

Gomes Da Cruz, L., Ishiyama, E. M., Boxler, C., Augustin, W., Scholl, S., & Wilson, D. I. (2015). Value pricing of surface coatings for mitigating heat exchanger fouling. *Food and Bioproducts Processing*, *93*(May), 343–363. https://doi.org/10.1016/j.fbp.2014.05.003

Goode, K. R., Asteriadou, K., Robbins, P. T., & Fryer, P. J. (2013). Fouling and cleaning studies in the food and beverage industry classified by cleaning type. *Comprehensive Reviews in Food Science and Food Safety*, *12*(2), 121–143. https://doi.org/10.1111/1541-4337.12000

Gordon, K. P., Hankinson, D. J., & Carver, C. E. (1968). Deposition of milk solids on heated surfaces. *Journal of Dairy Science*, *51*(4), 520–526. https://doi.org/10.3168/jds.S0022-0302(68)87022-5

Grasso, D., Subramaniam, K., Butkus, M., Strevett, K., & Bergendahl, J. (2002). A review of non-DLVO interactions in environmental colloidal systems. *Reviews in Environmental Science and Biotechnology*, *1*(1), 17–38. https://doi.org/10.1023/A:1015146710500

Grill, A. (1993). Review of the tribology of diamond-like carbon. *Wear*, *168*(1–2), 143–153. https://doi.org/10.1016/0043-1648(93)90210-D

Gudipati, C. S., Finlay, J. A., Callow, J. A., Callow, M. E., & Wooley, K. L. (2005). The antifouling and fouling-release performance of hyperbranched fluoropolymer (HBFP)-poly(ethylene glycol) (PEG) composite coatings evaluated by adsorption of biomacromolecules and the green fouling alga ulva. *Langmuir*, *21*(7), 3044–3053. https://doi.org/10.1021/la048015o

Guérin, R., Ronse, G., Bouvier, L., Debreyne, P., & Delaplace, G. (2007). Structure and rate of growth of whey protein deposit from in situ electrical conductivity during fouling in a plate heat exchanger. *Chemical Engineering Science*, *62*(7), 1948–1957. https://doi.org/10.1016/j.ces.2006.12.038

Hagsten, C. (2016). *Cleaning of ultra-high temperature milk fouling - Structural and compositional changes* (Vol. 7). Lund University.

Hagsten, C., Altskär, A., Gustafsson, S., Lorén, N., Hamberg, L., Innings, F., Paulsson, M., & Nylander, T. (2016). Composition and structure of high temperature dairy fouling. *Food Structure*, *7*, 13–20. https://doi.org/10.1016/j.foostr.2015.12.002

Hall, C. C. (1939). *The use of stainless steel in the food industry*. R.S.I, 741–753.

Hankinson, D. J., & Carver, C. E. (1968). Fluid dynamic relationships involved in circulation cleaning. *Journal of Dairy Science*, *51*(11), 1761–1767. https://doi.org/10.3168/jds.S0022-0302(68)87273-X

Hawkins, M. L., Faÿ, F., Réhel, K., Linossier, I., & Grunlan, M. A. (2014). Bacteria and diatom resistance of silicones modified with PEO-silane amphiphiles. *Biofouling*, *30*(2), 247–258. https://doi.org/10.1080/08927014.2013.862235

Hawkins, M. L., Schott, S. S., Grigoryan, B., Rufin, M. A., Ngo, B. K. D., VanderWal, L., Stafslien, S. J., & Grunlan, M. A. (2017). Anti-protein and anti-bacterial behavior of amphiphilic silicones. *Polymer Chemistry*, *8*(34), 5239–5251. https://doi.org/10.1039/c7py00944e

Hejda, F., Solaˇ, P., & Kousal, J. (2010). Surface free energy determination by contact angle measurements – A comparison of various approaches. *WDS'10 Proceedings of Contributed Papers*, *3*, 25–30.

Hinton, A. R., Trinh, K. T., Brooks, J. D., & Manderson, G. J. (2002). Thermophile survival in milk fouling and on stainless steel during cleaning. *Food and Bioproducts Processing: Transactions of the Institution of Chemical Engineers, Part C*, *80*(4), 299–304. https://doi.org/10.1205/096030802321154817

Hoffmann, M. A. M., & Van Mil, P. J. J. M. (1997). Heat-induced aggregation of β-lactoglobulin: Role of the free thiol group and disulfide bonds. *Journal of Agricultural and Food Chemistry*, *45*(8), 2942–2948. https://doi.org/10.1021/jf960789q

Holsinger, V. H., Rajkowski, K. T., & Stabel, J. R. (1997). Milk pasteurisation and safety: A brief history and update. *Revue Scientifique et Technique de l'OIE*, *16*(2), 441–451. https://doi.org/10.20506/rst.16.2.1037

Howell, C., Grinthal, A., Sunny, S., Aizenberg, M., & Aizenberg, J. (2018). Designing liquid-infused surfaces for medical applications: A review. *Advanced Materials*, *1802724*, 1–26. https://doi.org/10.1002/adma.201802724

Howell, C., Vu, T. L., Lin, J. J., Kolle, S., Juthani, N., Watson, E., Weaver, J. C., Alvarenga, J., & Aizenberg, J. (2014). Self-replenishing vascularized fouling-release surfaces. *ACS Applied Materials and Interfaces*, *6*(15), 13299–13307. https://doi.org/10.1021/am503150y

Hu, P., Xie, Q., Ma, C., & Zhang, G. (2020). Silicone-based fouling-release coatings for marine antifouling. *Langmuir*, *36*(9), 2170–2183. https://doi.org/10.1021/acs.langmuir.9b03926

Huang, K., & Goddard, J. M. (2015). Influence of fluid milk product composition on fouling and cleaning of Ni-PTFE modified stainless steel heat exchanger surfaces. *Journal of Food Engineering*, *158*, 22–29. https://doi.org/10.1016/j.jfoodeng.2015.02.026

Hucknall, A., Rangarajan, S., & Chilkoti, A. (2009). In pursuit of zero: Polymer brushes that resist the adsorption of proteins. *Advanced Materials*, *21*(23), 2441–2446. https://doi.org/10.1002/adma.200900383

Huo, J., Xiao, J., Kirk, T. V., & Chen, X. D. (2019). Effects of Fluorolink® S10 surface coating on WPC fouling of stainless steel surfaces and subsequent cleaning. *Food and Bioproducts Processing*, *118*, 130–138. https://doi.org/10.1016/j.fbp.2019.09.005

Itoh, H., Nagata, A., Toyomasu, T., Sakiyama, T., Nakanishi, K., Nagai, T., & Saeki, T. (1995). Adsorption of β-lactoglobulin onto the surface of stainless steel particles. *Bioscience, Biotechnology, and Biochemistry*, *59*(9), 1648–1651. https://doi.org/10.1271/bbb.59.1648

Jeevahan, J., Chandrasekaran, M., Britto Joseph, G., Durairaj, R. B., & Mageshwaran, G. (2018). Superhydrophobic surfaces: A review on fundamentals, applications, and challenges. *Journal of Coatings Technology and Research*, *15*(2), 231–250. https://doi.org/10.1007/s11998-017-0011-x

Jeurnink, T., Walstra, P., & De Kruif, C. (1996). Mechanisms of fouling in dairy processing. *Mechanisms of Fouling in Dairy Processing*, *50*(3), 407–426.

Jimenez, M., Delaplace, G., Nuns, N., Bellayer, S., Deresmes, D., Ronse, G., Alogaili, G., Collinet-Fressancourt, M., & Traisnel, M.

(2013). Toward the understanding of the interfacial dairy fouling deposition and growth mechanisms at a stainless steel surface: A multiscale approach. *Journal of Colloid and Interface Science*, *404*, 192–200. https://doi.org/10.1016/j.jcis.2013.04.021

Jimenez, M., Hamze, H., Allion, A., Ronse, G., Delaplace, G., & Traisnel, M. (2012). Antifouling stainless steel surface: Competition between roughness and surface energy. *Materials Science Forum*, *706–709*, 2523–2528. https://doi.org/10.4028/www.scientific.net/MSF.706-709.2523

Jing, X., & Guo, Z. (2019). Fabrication of biocompatible super stable lubricant-immobilized slippery surfaces by grafting a polydimethylsiloxane brush: Excellent boiling water resistance, hot liquid repellency and long-term slippery stability. *Nanoscale*, *11*(18), 8870–8881. https://doi.org/10.1039/c9nr01556f

Jovanović, B. (2015). Critical review of public health regulations of titanium dioxide, a human food additive. *Integrated Environmental Assessment and Management*, *11*(1), 10–20. https://doi.org/10.1002/ieam.1571

Kaelble, D. H. (1970). Dispersion-polar surface tension properties of organic solids. *The Journal of Adhesion*, *2*(2), 66–81. https://doi.org/10.1080/0021846708544582

Kananeh, A. B., Scharnbeck, E., Kück, U. D., & Räbiger, N. (2010). Reduction of milk fouling inside gasketed plate heat exchanger using nano-coatings. *Food and Bioproducts Processing*, *88*(4), 349–356. https://doi.org/10.1016/j.fbp.2010.09.010

Karlsson, C. A. C., Wahlgren, M. C., & Trägårdh, A. C. (1996). β-Lactoglobulin fouling and its removal upon rinsing and by SDS as influenced by surface characteristics, temperature and adsorption time. *Journal of Food Engineering*, *30*(1–2), 43–60. https://doi.org/10.1016/s0260-8774(96)00045-3

Khaldi, M., Croguennec, T., André, C., Ronse, G., Jimenez, M., Bellayer, S., Blanpain-Avet, P., Bouvier, L., Six, T., Bornaz, S., Jeantet, R., & Delaplace, G. (2018). Effect of the calcium/protein molar ratio on β-lactoglobulin denaturation kinetics and fouling phenomena. *International Dairy Journal*, *78*, 1–10. https://doi.org/10.1016/j.idairyj.2017.10.002

Kim, Y. D., Dordick, J. S., & Clark, D. S. (2001). Siloxane-based biocatalytic films and paints for use as reactive coatings. *Biotechnology and Bioengineering*, *72*(4), 475–482. https://doi.org/10.1002/1097-0290(20010220)72:4_475::AID-BIT1009_3.0.CO;2-F

Kirtley, S. A., & McGuire, J. (1989). On differences in surface constitution of dairy product contact materials. *Journal of Dairy Science*, *72*(7), 1748–1753. https://doi.org/10.3168/jds.S0022-0302(89)79291-2

Kumar, V., Pulpytel, J., Giudetti, G., Rauscher, H., Rossi, F., & Arefi-Khonsari, F. (2011). Amphiphilic copolymer coatings via plasma polymerisation process: Switching and anti-biofouling characteristics. *Plasma Processes and Polymers*, *8*(5), 373–385. https://doi.org/10.1002/ppap.201000109

Lalande, M., & Rene, F. (1988). Fouling by milk and dairy product and cleaning of heat exchange surfaces. In L. F. Melo, T. R. Bott, & C. A. Bernardo (Eds.), *Fouling science and technology* (pp. 557–573). Springer. https://doi.org/10.1007/978-94-009-2813-8_36

Lalande, M., Rene, F., & Tissier, J. P. (1989). Fouling and its control in heat exchangers in the dairy industry. *Biofouling*, *1*(3), 233–250. https://doi.org/10.1080/08927018909378111

Lalande, M., Tissier, J., & Corrieu, G. (1985). Fouling of heat transfer surfaces related to β-lactoglobulin denaturation during heat processing of milk. *Biotechnology Progress*, *1*(2), 131–139. https://doi.org/10.1002/btpr.5420010210

Leonardi, A. K., & Ober, C. K. (2019). Polymer-Based marine antifouling and fouling release surfaces: Strategies for synthesis and modification. *Annual Review of Chemical and Biomolecular Engineering*, *10*(1), 241–264. https://doi.org/10.1146/annurev-chembioeng-060718-030401

Liu, D. Z., Jindal, S., Amamcharla, J., Anand, S., & Metzger, L. (2017). Short communication: Evaluation of a sol-gel–based stainless steel surface modification to reduce fouling and biofilm formation during pasteurization of milk. *Journal of Dairy Science*, *100*(4), 2577–2581. https://doi.org/10.3168/jds.2016-12141

Liu, W., Chen, X. D., Jeantet, R., André, C., Bellayer, S., & Delaplace, G. (2020). Effect of casein/whey ratio on the thermal denaturation of whey proteins and subsequent fouling in a plate heat exchanger. *Journal of Food Engineering*, *289*, 110175. https://doi.org/10.1016/j.jfoodeng.2020.110175

Liu, Y., Zou, Y., Zhao, L., Liu, W., & Cheng, L. (2011). Investigation of adhesion of CaCO3 crystalline fouling on stainless steel surfaces with different roughness. *International Communications in Heat and Mass Transfer*, *38*(6), 730–733. https://doi.org/10.1016/j.icheatmasstransfer.2011.04.003

Lyster, R. L. J. (1965). The composition of milk deposits in an U.H.T. plant. *Journal of Dairy Research*, *32*(1), 203–208.

Ma, H., Hyun, J., Stiller, P., & Chilkoti, A. (2004). Non-fouling" Oligo(ethylene glycol)-functionalized polymer brushes synthesized by surface-initiated atom transfer radical polymerization. *Advanced Materials*, *16*(4), 338–341. https://doi.org/10.1002/adma.200305830

Magens, O. M. (2019). *Mitigating fouling of heat exchangers with fluoropolymer coatings*. University of Cambridge.

Magens, O. M., Ishiyama, E. M., & Wilson, D. I. (2016). Quantifying the "implementation gap" for antifouling coatings. *Applied Thermal Engineering*, *99*, 683–689. https://doi.org/10.1016/j.applthermaleng.2016.01.087

Mahdi, Y., Mouheb, A., & Oufer, L. (2009). A dynamic model for milk fouling in a plate heat exchanger. *Applied Mathematical Modelling*, *33*(2), 648–662. https://doi.org/10.1016/j.apm.2007.11.030

Manabe, K., Kyung, K. H., & Shiratori, S. (2015). Biocompatible slippery fluid-infused films composed of chitosan and alginate via layer-by-layer self-assembly and their antithrombogenicity. *ACS Applied Materials and Interfaces*, *7*(8), 4763–4771. https://doi.org/10.1021/am508393n

Manna, U., & Lynn, D. M. (2015). Fabrication of liquid-infused surfaces using reactive polymer multilayers: Principles for manipulating the behaviors and mobilities of aqueous fluids on slippery liquid interfaces. *Advanced Materials*, *27*(19), 3007–3012. https://doi.org/10.1002/adma.201500893

Marchand, S., De Block, J., De Jonghe, V., Coorevits, A., Heyndrickx, M., & Herman, L. (2012). Biofilm formation in milk production and processing environments; influence on milk quality and safety. *Comprehensive Reviews in Food Science and Food Safety*, *11*(2), 133–147. https://doi.org/10.1111/j.1541-4337.2011.00183.x

Mauermann, M., Eschenhagen, U., Bley, T., & Majschak, J. P. (2009). Surface modifications - Application potential for the reduction of cleaning costs in the food processing industry. *Trends in Food Science and Technology*, *20*(SUPPL. 1), S9–S15. https://doi.org/10.1016/j.tifs.2009.01.020

Mayer, J. W., Eriksson, L., & Davies, J. A. (1970). *Ion implantation in semiconductors: Silicon and germanium*. Academic Press.

McGuire, J., & Swartzel, K. R. (1989). The influence of solid surface energetics on macromolecular adsorption from milk. *Journal of Food Processing and Preservation*, *13*(2), 145–160. https://doi.org/10.1111/j.1745-4549.1989.tb00097.x

McHale, G., Shirtcliffe, N. J., & Newton, M. I. (2004). Contact-angle hysteresis on super-hydrophobic surfaces. *Langmuir*, *20*(23), 10146–10149. https://doi.org/10.1021/la0486584

Mérian, T., & Goddard, J. M. (2012). Advances in nonfouling materials: Perspectives for the food industry. *Journal of Agricultural and Food Chemistry*, *60*(12), 2943–2957. https://doi.org/10.1021/jf204741p

Müller-Steinhagen, H., & Zhao, Q. (1997). Investigation of low fouling surface alloys made by ion implantation technology. *Chemical Engineering Science*, *52*(19), 3321–3332. https://doi.org/10.1016/S0009-2509(97)00162-0

Ndoye, F. T., Erabit, N., Flick, D., & Alvarez, G. (2013). In-line characterization of a whey protein aggregation process: Aggregates size and rheological measurements. *Journal of Food Engineering*, *115*(1), 73–82. https://doi.org/10.1016/j.jfoodeng.2012.09.021

Nishioka, S., Tenjimbayashi, M., Manabe, K., Matsubayashi, T., Suwabe, K., Tsukada, K., & Shiratori, S. (2016). Facile design of plant-oil-infused fine surface asperity for transparent blood-repelling endoscope lens. *RSC Advances*, *6*(53), 47579–47587. https://doi.org/10.1039/c6ra08390k

Owens, D. K., & Wendt, R. C. (1969). Estimation of the surface free energy of polymers. *Journal of Applied Polymer Science*, *13*(8), 1741–1747. https://doi.org/10.1002/app.1969.070130815

Patel, J. S., Bansal, B., Jones, M. I., & Hyland, M. (2013). Fouling behaviour of milk and whey protein isolate solution on doped diamond-like carbon modified surfaces. *Journal of Food Engineering*, *116*(2), 413–421. https://doi.org/10.1016/j.jfoodeng.2012.12.014

Petit, J., Herbig, A. L., Moreau, A., & Delaplace, G. (2011). Influence of calcium on β-lactoglobulin denaturation kinetics: Implications in unfolding and aggregation mechanisms. *Journal of Dairy Science*, *94*(12), 5794–5810. https://doi.org/10.3168/jds.2011-4470

Petit, J., Six, T., Moreau, A., Ronse, G., & Delaplace, G. (2013). β-Lactoglobulin denaturation, aggregation, and fouling in a plate heat exchanger: Pilot-scale experiments and dimensional analysis. *Chemical Engineering Science*, *101*, 432–450. https://doi.org/10.1016/j.ces.2013.06.045

Piepiórka Stepuk, J., Tandecka, K., & Jakubowski, M. (2016). An analysis of milk fouling formed during heat treatment on a stainless steel surface with different degrees of roughness. *Czech Journal of Food Sciences*, *34*(3), 271–279. https://doi.org/10.17221/466/2015-CJFS

Polat, Z. (2009). *Integrated approach to whey utilization through natural zeolite adsorption/desorption and fermentation*. Institute of Technology of Izmir.

Premathilaka, S., Hyland, M., Chen, X., & Bansal, B. (2006). A study of the effects of surface chemistry on the initial deposition mechanisms of dairy fouling. *Food and Bioproducts Processing*, *84*(4 C), 265–273. https://doi.org/10.1205/fbp06026

Premathilaka, S. S., Hyland, M. M., Chen, X. D., Watkins, L. R., & Bansal, B. (2007). Interaction of whey protein with modified stainless steel surfaces. In H. Müller-Steinhagen, M. Reza Malayeri, & A. Paul Watkinson (Eds.), *Heat exchanger fouling and cleaning - Challenges and opportunities*. Engineering Conferences International. http://dc.engconfintl.org/cgi/viewcontent.cgi?article=1020&context=heatexchanger2007

Robbins, P. T., Elliott, B. L., Fryer, P. J., Belmar, M. T., & Hasting, A. P. M. (1999). A comparison of milk and whey fouling in a pilot scale plate heat exchanger: Implications for modelling and mechanistic studies. *Food and Bioproducts Processing: Transactions of the Institution of Chemical Engineers, Part C*, *77*(2), 97–106. https://doi.org/10.1205/096030899532385

Robertson, J. (2002). Diamond-like amorphous carbon. *Materials Science and Engineering: R: Reports*, *37*(4–6), 129–281. https://doi.org/10.1016/s0927-796x(02)00005-0

Rosmaninho, R., & Melo, L. F. (2006). Calcium phosphate deposition from simulated milk ultrafiltrate on different stainless steel-based surfaces. *International Dairy Journal*, *16*(1), 81–87. https://doi.org/10.1016/j.idairyj.2005.01.006

Rosmaninho, R., & Melo, L. F. (2007). Effect of proteins on calcium phosphate deposition in turbulent flow as a function of surface properties. *Experimental Thermal and Fluid Science*, *32*(2), 375–386. https://doi.org/10.1016/j.expthermflusci.2007.04.012

Rosmaninho, R., & Melo, L. F. (2008). Protein-calcium phosphate interactions in fouling of modified stainless-steel surfaces by simulated milk. *International Dairy Journal*, *18*(1), 72–80. https://doi.org/10.1016/j.idairyj.2007.06.008

Rosmaninho, R., Rizzo, G., Müller-Steinhagen, H., & Melo, L. F. (2008). Deposition from a milk mineral solution on novel heat transfer surfaces under turbulent flow conditions. *Journal of Food Engineering*, *85*(1), 29–41. https://doi.org/10.1016/j.jfoodeng.2007.06.018

Rosmaninho, R., Rizzo, G., Müller-Steinhagen, H., & Melo, L. F. (2003). Study of the influence of bulk properties and surface tension on the deposition process of calcium phosphate on modified stainless steel. In M. R. M. P. Watkinson & H. Müller-Steinhagen (Eds.), *Heat exchanger fouling and cleaning: Fundamentals and applications*. Engineering Conferences International.

Rosmaninho, R., Santos, O., Nylander, T., Paulsson, M., Beuf, M., Benezech, T., Yiantsios, S., Andritsos, N., Karabelas, A., Rizzo, G., Müller-Steinhagen, H., & Melo, L. F. (2007). Modified stainless steel surfaces targeted to reduce fouling - Evaluation of fouling by milk components. *Journal of Food Engineering*, *80*(4), 1176–1187. https://doi.org/10.1016/j.jfoodeng.2006.09.008

Rufin, M. A., Barry, M. E., Adair, P. A., Hawkins, M. L., Raymond, J. E., & Grunlan, M. A. (2016). Protein resistance efficacy of PEO-silane amphiphiles: Dependence on PEO-segment length and concentration. *Acta Biomaterialia*, *41*, 247–252. https://doi.org/10.1016/j.actbio.2016.04.020

Rufin, M. A., Gruetzner, J. A., Hurley, M. J., Hawkins, M. L., Raymond, E. S., Raymond, J. E., & Grunlan, M. A. (2015). Enhancing the protein resistance of silicone via surface-restructuring PEO-silane amphiphiles with variable PEO length. *Journal of Materials Chemistry B*, *3*(14), 2816–2825. https://doi.org/10.1039/c4tb02042a

Rungraeng, N., Cho, Y. C., Yoon, S. H., & Jun, S. (2012). Carbon nanotube-polytetrafluoroethylene nanocomposite coating for milk fouling reduction in plate heat exchanger. *Journal of Food Engineering*, *111*(2), 218–224. https://doi.org/10.1016/j.jfoodeng.2012.02.032

Sadeghinezhad, E., Kazi, S. N., Badarudin, A., Zubair, M. N. M., Dehkordi, B. L., & Oon, C. S. (2013). A review of milk fouling on heat exchanger surfaces. *Reviews in Chemical Engineering*, *29*(3), 169–188. https://doi.org/10.1515/revce-2013-0003

Sadeghinezhad, E., Kazi, S. N., Dahari, M., Safaei, M. R., Sadri, R., & Badarudin, A. (2015). A comprehensive review of milk fouling on heated surfaces. *Critical Reviews in Food Science and Nutrition*, *55*(12), 1724–1743. https://doi.org/10.1080/10408398.2012.752343

Santos, O., Nylander, T., Rosmaninho, R., Rizzo, G., Yiantsios, S., Andritsos, N., Karabelas, A., Müller-Steinhagen, H., Melo, L., Boulangé-Petermann, L., Gabet, C., Braem, A., Trägårdh, C., & Paulsson, M. (2004). Modified stainless steel surfaces targeted to reduce fouling - Surface characterization. *Journal of Food Engineering*, *64*(1), 63–79. https://doi.org/10.1016/j.jfoodeng.2003.09.013

Santos, O., Nylander, T., Schillén, K., Paulsson, M., & Trägårdh, C. (2006). Effect of surface and bulk solution properties on the adsorption of whey protein onto steel surfaces at high temperature. *Journal of Food Engineering*, *73*(2), 174–189. https://doi.org/10.1016/j.jfoodeng.2005.01.018

Schmidt, R. H., Erickson, D. J., Sims, S., & Wolff, P. (2012). Characteristics of food contact surface materials: Stainless steel. *Food Protection Trends*, *32*(10), 574–584.

Schnöing, L., Augustin, W., & Scholl, S. (2020). Fouling mitigation in food processes by modification of heat transfer surfaces: A review. *Food and Bioproducts Processing*, *121*, 1–19. https://doi.org/10.1016/j.fbp.2020.01.013

Scudeller, L. A., Blanpain-Avet, P., Six, T., Bellayer, S., Jimenez, M., Croguennec, T., André, C., & Delaplace, G. (2021). Calcium chelation by phosphate ions and its influence on fouling mechanisms of whey protein solutions in a plate heat exchanger. *Foods*, *10*(2), 259.

Simmons, M. J. H., Jayaraman, P., & Fryer, P. J. (2007). The effect of temperature and shear rate upon the aggregation of whey protein and its implications for milk fouling. *Journal of Food Engineering*, *79*(2), 517–528. https://doi.org/10.1016/j.jfoodeng.2006.02.013

Smithers, G. W., Ballard, F. J., Copeland, A. D., De Silva, K. J., Dionysius, D. A., Francis, G. L., Goddard, C., Grieve, P. A., Mcintosh, G. H., Mitchell, I. R., John Pearce, R., & Regester, G. O. (1996). New opportunities from the isolation and utilization of whey proteins. *Journal of Dairy Science*, *79*(8), 1454–1459. https://doi.org/10.3168/jds.S0022-0302(96)76504-9

Sundaram, H. S., Cho, Y., Dimitriou, M. D., Weinman, C. J., Finlay, J. A., Cone, G., Callow, M. E., Callow, J. A., Kramer, E. J., & Ober, C. K. (2011). Fluorine-free mixed amphiphilic polymers based on PDMS and PEG side chains for fouling release applications. *Biofouling*, *27*(6), 589–602. https://doi.org/10.1080/08927014.2011.587662

Timperley, D. A., & Smeulders, C. N. M. (1987). Cleaning of dairy HTST plate heat exchangers: Comparison of single- and two-stage procedures. *International Journal of Dairy Technology*, *40*(1), 4–7. https://doi.org/10.1111/j.1471-0307.1987.tb02383.x

Timperley, D. A., & Smeulders, C. N. M. (1988). Cleaning of dairy HTST plate heat exchangers: Optimization of the single-stage procedure. *International Journal of Dairy Technology*, *41*(1), 4–7. https://doi.org/10.1111/j.1471-0307.1988.tb00572.x

Tissier, J. P., & Lalande, M. (1986). Experimental device and methods for studying milk deposit formation on heat exchange surfaces. *Biotechnology Progress*, *2*(4), 218–229. https://doi.org/10.1002/btpr.5420020410

Togasawa, R., Tenjimbayashi, M., Matsubayashi, T., Moriya, T., Manabe, K., & Shiratori, S. (2018). A fluorine-free slippery surface with hot water repellency and improved stability against boiling. *ACS Applied Materials and Interfaces*, *10*(4), 4198–4205. https://doi.org/10.1021/acsami.7b15689

Trojan, K., Grischke, M., & Dimigen, H. (1994). Network modification of DLC coatings to adjust a defined surface energy. *Physica Status Solidi (A)*, *145*(2), 575–585. https://doi.org/10.1002/pssa.2211450242

Van Asselt, A. J., Vissers, M. M., Smit, F., & De Jong, P. (2005). *In-line control of fouling*. Proceedings of Heat Exchanger Fouling and Cleaning: Challenges and Opportunities.

van Oss, C. J. (1995). Hydrophobicity of biosurfaces - Origin, quantitative determination and interaction energies. *Colloids and Surfaces B: Biointerfaces*, *5*(3–4), 91–110. https://doi.org/10.1016/0927-7765(95)01217-7

van Oss, C. J. (2006). *Interfacial forces in aqueous media* (2nd ed.). CRC Press. https://doi.org/10.1016/j.actbio.2009.08.002.In

Van Oss, C. J. (2003). Long-range and short-range mechanisms of hydrophobic attraction and hydrophilic repulsion in specific and aspecific interactions. *Journal of Molecular Recognition*, *16*(4), 177–190. https://doi.org/10.1002/jmr.618

van Oss, C. J., Chaudhury, M. K., & Good, R. J. (1988). Interfacial Lifshitz-van der Waals and polar interactions in macroscopic systems. *Chemical Reviews*, *88*(6), 927–941. https://doi.org/10.1021/cr00088a006

Van Oss, C. J., Good, R. J., & Chaudhury, M. K. (1987). Determination of the hydrophobic interaction energy-application to separation processes. *Separation Science and Technology*, *22*(1), 1–24. https://doi.org/10.1080/01496398708056155

Verran, J., & Redfern, J. (2016). Testing surface cleanability in food processing. In H. Lelieveld, J. Holah, & D. Gabrić (Eds.), *Handbook of hygiene control in the food industry* (2nd ed., pp. 651–661). Elsevier. https://doi.org/10.1016/B978-0-08-100155-4.00042-X

Verwey, E. J. W., & Overbeek, J. T. G. (1948). *Theory of the stability of lyophobic colloids*. Elsevier.

Visser, J., & Jeurnink, T. J. M. (1997). Fouling of heat exchangers in the dairy industry. *Experimental Thermal and Fluid Science*, *14*(4), 407–424. https://doi.org/10.1016/S0894-1777(96)00142-2

Walstra, P., Wouters, J. T. M., & Geurts, T. J. (2005). *Dairy science and technology* (Vol. 2). Taylor & Francis.

Wei, J., Ravn, D. B., Gram, L., & Kingshott, P. (2003). Stainless steel modified with poly(ethylene glycol) can prevent protein adsorption but not bacterial adhesion. *Colloids and Surfaces B: Biointerfaces*, *32*(4), 275–291. https://doi.org/10.1016/S0927-7765(03)00180-2

Wenzel, R. N. (1936). Resistance of solid surfaces to wetting by water. *Industrial and Engineering Chemistry*, *28*(8), 988–994. https://doi.org/10.1021/ie50320a024

Wolz, M., Mersch, E., & Kulozik, U. (2016). Thermal aggregation of whey proteins under shear stress. *Food Hydrocolloids*, *56*, 396–404. https://doi.org/10.1016/j.foodhyd.2015.12.036

Wong, T. S., Kang, S. H., Tang, S. K. Y., Smythe, E. J., Hatton, B. D., Grinthal, A., & Aizenberg, J. (2011). Bioinspired self-repairing slippery surfaces with pressure-stable omniphobicity. *Nature*, *477*(7365), 443–447. https://doi.org/10.1038/nature10447

Wu, S. (1973). Polar and nonpolar interactions in adhesion. *The Journal of Adhesion*, *5*(1), 39–55. https://doi.org/10.1080/00218467308078437

Yan, Y. Y., Gao, N., & Barthlott, W. (2011). Mimicking natural superhydrophobic surfaces and grasping the wetting process: A review on recent progress in preparing superhydrophobic surfaces. *Advances*

in Colloid and Interface Science, *169*(2), 80–105. https://doi.org/10.1016/j.cis.2011.08.005

Yoon, J., & Lund, D. B. (1994). Magnetic treatment of milk and surface treatment of plate heat exchangers: Effects on milk fouling. *Journal of Food Science*, *59*(5), 964–969. https://doi.org/10.1111/j.1365-2621.1994.tb08168.x

Young, T. (1804). An essay to the cohesion of fluids. *Philosophical Transaction of the Royal Society of London*, 65–87.

Zhang, C., Xia, Y., Zhang, H., & Zacharia, N. S. (2018). Surface functionalization for a nontextured liquid-infused surface with enhanced lifetime. *ACS Applied Materials and Interfaces*, *10*(6), 5892–5901. https://doi.org/10.1021/acsami.7b18021

Zhang, G., Liang, B., Zhong, Z., Huang, Y., & Su, Z. (2018). One-step solvent-free strategy for covalently attached, substrate-independent transparent slippery coating. *Advanced Materials Interfaces*, *5*(20), 1–7. https://doi.org/10.1002/admi.201800646

Zhao, Q., & Burnside, B. M. (1994). Dropwise condensation of steam on ion implanted condenser surfaces. *Heat Recovery Systems & CHP*, *14*(5), 525–534.

Zhao, Q., Liu, C., & Liu, Y. (2007). *Bacterial and protein adhesion on NI-P-PTFE coated surfaces*. ECI Symposium Series Heat Exchanger Fouling and Cleaning VI, 237. http://services.bepress.com/eci/heatexchanger2007/33/

Zhao, Q., Liu, Y., Wang, C., Wang, S., & Müller-Steinhagen, H. (2005). Effect of surface free energy on the adhesion of biofouling and crystalline fouling. *Chemical Engineering Science*, *60*(17), 4858–4865. https://doi.org/10.1016/j.ces.2005.04.006

Zhao, Q., & Müller-Steinhagen, H. (2001). *Intermolecular and adhesion forces of deposits on modified heat transfer surfaces*. Proceedings of Heat Exchanger Fouling, Fundamental Approaches and Technical Solutions.

Zhao, Q., Wang, S., & Müller-Steinhagen, H. (2004). Tailored surface free energy of membrane diffusers to minimize microbial adhesion. *Applied Surface Science*, *230*(1–4), 371–378. https://doi.org/10.1016/j.apsusc.2004.02.052

Zhou, Z., Calabrese, D. R., Taylor, W., Finlay, J. A., Callow, M. E., Callow, J. A., Fischer, D., Kramer, E. J., & Ober, C. K. (2014). Amphiphilic triblock copolymers with PEGylated hydrocarbon structures as environmentally friendly marine antifouling and fouling-release coatings. *Biofouling*, *30*(5), 589–604. https://doi.org/10.1080/08927014.2014.897335

Zisman, W. A. (1964). Relation of the equilibrium contact angle to liquid and solid constitution. In F. M. Fowkes (Ed.), *Contact angle, wettability, and adhesion* (Vol. 51, pp. 1–51). American Chemical Society. https://doi.org/10.1021/ba-1964-0043.ch001

Zouaghi, S. (2018). *Dairy fouling on stainless steel and design of antifouling surfaces*. Université de Lille.

Zouaghi, S., Abdallah, M., André, C., Chihib, N. E., Bellayer, S., Delaplace, G., Celzard, A., & Jimenez, M. (2018). Graphite-based composites for whey protein fouling and bacterial adhesion management. *International Dairy Journal*, *86*, 69–75. https://doi.org/10.1016/j.idairyj.2018.07.004

Zouaghi, S., Barry, M. E., Bellayer, S., Lyskawa, J., André, C., Delaplace, G., Grunlan, M. A., & Jimenez, M. (2018). Antifouling amphiphilic silicone coatings for dairy fouling mitigation on stainless steel. *Biofouling*, *34*(7), 769–783. https://doi.org/10.1080/08927014.2018.1502275

Zouaghi, S., Frémiot, J., André, C., Grunlan, M. A., Gruescu, C., Delaplace, G., Duquesne, S., & Jimenez, M. (2019). Investigating the effect of an antifouling surface modification on the environmental impact of a pasteurization process: An LCA study. *ACS Sustainable Chemistry and Engineering*, *7*(10), 9133–9142. https://doi.org/10.1021/acssuschemeng.8b05835

Zouaghi, S., Six, T., Bellayer, S., Coffinier, Y., Abdallah, M., Chihib, N. E., André, C., Delaplace, G., & Jimenez, M. (2018). Atmospheric pressure plasma spraying of silane-based coatings targeting whey protein fouling and bacterial adhesion management. *Applied Surface Science*, *455*(February), 392–402. https://doi.org/10.1016/j.apsusc.2018.06.006

Zouaghi, S., Six, T., Bellayer, S., Moradi, S., Hatzikiriakos, S. G., Dargent, T., Thomy, V., Coffinier, Y., André, C., Delaplace, G., & Jimenez, M. (2017). Antifouling biomimetic liquid-infused stainless steel: Application to dairy industrial processing. *ACS Applied Materials and Interfaces*, *9*(31), 26565–26573. https://doi.org/10.1021/acsami.7b06709

Zouaghi, S., Six, T., Nuns, N., Simon, P., Bellayer, S., Moradi, S., Hatzikiriakos, S. G., André, C., Delaplace, G., & Jimenez, M. (2018). Influence of stainless steel surface properties on whey protein fouling under industrial processing conditions. *Journal of Food Engineering*, *228*, 38–49. https://doi.org/10.1016/j.jfoodeng.2018.02.009

Zúñiga, R. N., Tolkach, A., Kulozik, U., & Aguilera, J. M. (2010). Kinetics of formation and physicochemical characterization of thermally-induced β-Lactoglobulin aggregates. *Journal of Food Science*, *75*(5), E261–E268. https://doi.org/10.1111/j.1750-3841.2010.01617.x

How to cite this article: Saget, M., de Almeida, C. F., Fierro, V., Celzard, A., Delaplace, G., Thomy, V., Coffinier, Y., & Jimenez, M. A critical review on surface modifications mitigating dairy fouling. *Compr Rev Food Sci Food Saf*, 2021;*20:*4324–4366. https://doi.org/10.1111/1541-4337.12794